

THESIS

STUDYING AGE-RELATED CHANGES IN WHITE MATTER MICROSTRUCTURE IN  
HEALTHY AGING USING NONINVASIVE MRI TECHNIQUES.

Submitted by

Andrea Mendez Colmenares

Department of Psychology

In partial fulfillment of the requirements

For the Degree of Master of Science

Colorado State University

Fort Collins, Colorado

Spring 2020

Master's Committee:

Advisor: Michael L. Thomas

Agnieszka Z. Burzynska

Donald C. Rojas

Copyright by Andrea Mendez Colmenares 2020

All Rights Reserved

## ABSTRACT

### STUDYING AGE-RELATED CHANGES IN WHITE MATTER MICROSTRUCTURE IN HEALTHY AGING USING NONINVASIVE MRI TECHNIQUES.

Age-related deterioration of the white matter (WM), such as demyelination, is an important mechanism of cognitive decline in healthy aging. Lifestyle factors can influence the course of WM aging. Most evidence have used diffusion tensor imaging (DTI) metrics, but these are not specific to myelin or axons. Therefore, in this study we compared DTI metrics to a proposed proxy of myelin content, the T1-weighted image (T1-WI) to T2-weighted image (T2-WI) ratio with respect to their ability to: detect time-by-intervention interactions, predict processing speed ability, and their correlations with each other and age. We used longitudinal data from 169 cognitively healthy older adults (60-79yrs). MRI imaging (3T Siemens Trio) included 0.9mm<sup>3</sup> MPRAGE, 1.7×1.7×3mm<sup>3</sup> T2w and DTI (30 diff. dir., bval= 0 and 1000s/mm<sup>2</sup>, 1.7×1.7×3mm<sup>3</sup>). T1w/T2w was calculated using internal intensity calibration. We used FSL-FDT to extract DTI metrics, focused on major WM tracts using tract-based spatial statistics in FSL. From the WM skeleton, we calculated mean values for 12 regions-of-interest. Processing speed was assessed using the Virginia Cognitive Aging Battery. Results showed that the T1w/T2w produced greater time-by-intervention interactions than DTI-FA, especially in the posterior ( $\beta=0.27$ ,  $p=0.01$ ) and anterior ( $\beta=0.33$ ,  $p=0.01$ ) limb of the internal capsule. The T1w/T2w (in the whole WM) correlated with processing speed ( $\beta=-0.13$ ,  $p=0.02$ ). T1w/T2w correlated with DTI in regions with high fiber coherence/high myelin content; and with age in regions with high myelin content. Results suggest that the T1w/T2w offers greater ability than

DTI to detect short-term longitudinal changes in WM, but they seem to reflect different microstructural properties in the WM. Further research is needed to gain a better understanding of its biological underpinnings and significance.

## TABLE OF CONTENTS

ABSTRACT.....	ii
1. CHAPTER 1: INTRODUCTION.....	1
1.1. DIFFUSION TENSOR IMAGING .....	1
1.2. AGING WHITE MATTER .....	4
1.3. LIFESTYLE AND WHITE MATTER AGING.....	7
1.4. CONVENTIONAL MRI METHODS .....	9
1.5. OVERVIEW OF THE CURRENT STUDY .....	12
2. CHAPTER 2: METHODS.....	14
2.1. STUDY SAMPLE .....	14
2.2. INTERVENTION.....	15
2.3. MRI ACQUISITION .....	16
2.4. MRI PREPROCESSING .....	16
2.5. T1W/T2W RATIO CALCULATION .....	18
2.6. REGIONS-OF-INTEREST.....	19
2.7. STATISTICAL ANALYSES .....	22
3. CHAPTER 3: RESULTS.....	24
3.1. INTERVENTION EFFECTS .....	25
3.2. ASSOCIATIONS WITH PROCESSING SPEED .....	26
3.3. ASSOCIATIONS BETWEEN DTI AND T1W/T2W.....	28
3.4. CORRELATIONS WITH AGE .....	29
3.5. T1W/T2W AND FA VALUES IN WHITE MATTER VS GREY MATTER .....	31
4. CHAPTER 4: DISCUSSION.....	32
4.1. WHITE MATTER AND MYELIN PLASTICITY .....	32
4.2. MOLECULAR PATHWAYS LINKING EXERCISE AND WM INTEGRITY .....	33
4.3. IN-VIVO WM IMAGING AND INTERVENTION EFFECTS .....	33
4.4. PROCESSING SPEED AND T1W/T2W.....	35
4.5. ASSOCIATIONS BETWEEN DTI AND T1W/T2W.....	37
4.6. CORRELATIONS BETWEEN T1W/T2W AND AGE.....	38
4.7. INTERPRETATION OF THE T1W/T2W SIGNAL. IS IT MYELIN?.....	40
4.8. CONCLUSIONS AND LIMITATIONS .....	40
REFERENCES .....	43
APPENDIX A.....	61
APPENDIX B .....	62
APPENDIX C .....	63

## 1. CHAPTER 1: INTRODUCTION

Human white matter (WM) is largely composed of myelinated axons. Properties of WM determine the speed of signal conduction and the precise timing in the transduction and transmission of neural signals (Chorghay, Káradóttir, & Ruthazer, 2018). The deterioration of WM is thought to result in disrupted communication among distributed grey matter regions—the “disconnection hypothesis”—which is considered to be one of the key mechanisms underlying cognitive decline in healthy aging and dementia (Bartzokis, 2004; O’Sullivan et al., 2001). Histopathological age-related changes in WM include myelin breakdown (Scheltens et al., 1995), axonal loss, and gliosis (Peters, 2002a), which may result in a significantly lower axonal conduction velocity. In addition, WM changes can be associated with cerebral microvascular damage, which leads to cerebral hypoperfusion, axonal damage, and demyelination (Washida, Hattori, & Ihara, 2019). However, the above evidence comes mostly from *post-mortem* human and non-human primates – much less is known about WM in living humans. This thesis explores new avenues in noninvasive MRI techniques used to study age-related changes in WM microstructure.

### 1.1. Diffusion Tensor Imaging

Diffusion tensor imaging (DTI) is a methodology used to measure the magnitude and orientation of water diffusion in biological tissues (Pierpaoli & Basser, 1996; Tournier, Mori, & Leemans, 2011). DTI was developed in the early 1990s. Since then, DTI has been the “gold standard” noninvasive technique for studying WM macrostructure *in vivo*.

A mathematical model to describe this process, termed the diffusion tensor (Pierpaoli & Basser, 1996), uses a 3 x 3 symmetric matrix, and vector bases, to describe the degree and

direction of diffusion displacement over time. The geometric shape associated with the diffusion tensor is a 3D ellipsoid which can be decomposed into basic geometric measures.

Diagonalization of the diffusion tensor elements derives three eigenvalues ( $\lambda_1$ ,  $\lambda_2$  and  $\lambda_3$ ) and their eigenvectors ( $\epsilon_1$ ,  $\epsilon_2$  and  $\epsilon_3$ ). Eigenvectors define the principal directions of diffusion along the axes of the ellipsoid, and eigenvalues define the length (radius) of each principal axis of the ellipsoid (Basser, Mattiello, & LeBihan, 1994).

From these eigenvectors and eigenvalues, we can calculate several metrics of interest in each brain voxel. The first is the directionality of motion of water molecules, which is commonly quantified using fractional anisotropy (FA):

$$FA = \frac{\sqrt{(\lambda_1 - \lambda_2)^2 + (\lambda_2 - \lambda_3)^2 + (\lambda_1 - \lambda_3)^2}}{\sqrt{2(\lambda_1^2 + \lambda_2^2 + \lambda_3^2)}}, \quad \text{EQ.1}$$

where the  $\lambda$ s are the eigenvalues describing the diffusion tensor. In tissues where there is no preferred direction for diffusion, as in gray matter or cerebrospinal fluid, FA is low and near zero. In contrast, in tissues with a higher degree of directional restriction of diffusion, FA is high (Alexander, Lee, Lazar, & Field, 2007). Because WM is composed of condensed, highly organized axonal fibers, the molecular diffusion of water in WM tracts usually demonstrates high FA, particularly in compact fiber tracts, such as the anterior corpus callosum.

Another measure of diffusivity is mean diffusivity (MD), which measures the average of the eigenvalues and indicates the overall magnitude of diffusion within a voxel. The magnitude of diffusion is determined by microstructural elements that may hinder diffusion in any direction, such as density and permability of cellular membranes. Radial diffusivity (RD), on the other hand, is a measure of the magnitude of diffusion perpendicular to the main orientation of the

WM tracts. Thus, RD has been often considered as a proxy of myelin content and axonal damage (Song et al., 2003, 2002b).

Anisotropy has previously been assumed to be an indirect measure of the integrity of myelinated axons in the brain (Kochunov et al., 2012). However, the interpretation of the neurobiological mechanisms of altered FA is not straightforward. In WM, most axons do not run in parallel within a voxel, and about 60-90% of WM voxels contain crossing fibers (Mädler, Drabycz, Kolind, Whittall, & MacKay, 2008), lowering FA values even in regions where the axonal integrity is intact. In addition, cellular and molecular processes that determine FA vary across brain regions. These processes include axonal integrity, permeability of axonal membranes, cytoplasmic transport and enlargement of extracellular spaces (ref). Therefore, the degree of anisotropy alone cannot discriminate between microstructural geometry and integrity of different WM microstructural elements (Jones, Knösche, & Turner, 2013).

## **1.2. Aging White Matter**

Histopathological studies have revealed that the age-related deterioration of WM is marked by degradation of myelin (Peters, 2002b), thinner myelin fibers (Marnier, Nyengaard, Tang, & Pakkenberg, 2003), decrease in axon caliber (Mason, Langaman, Morell, Suzuki, & Matsushima, 2001), formation of redundant myelin (Peters, 2002b) and abnormalities in oligodendrocytes (myelinating cells) lineage (Tse & Herrup, 2017). Most of the evidence on WM deterioration comes from studies on rodents or non-human primates. However, there are very different scaling rules of WM expansion across mammalian orders (Kuhn, Gritti, Crooks, & Dombrowski, 2019). For example, in the human brain, it is the volume of WM that shows the largest difference between human and non-human primates (Schoenemann, Sheehan, & Glotzer, 2005). Studies of non-human primates have found that, in contrast to humans, the WM volumes

remain stable with advancing age, with a subtle volume loss of the prefrontal cortex and no change in other brain regions like the hippocampus (Sherwood et al., 2011). This is important, since the hippocampus and the prefrontal WM are brain regions vulnerable to aging in humans (Raz et al., 2005). Despite the important evidence that animal studies have added to the understanding of WM, there are differences that need to be accounted when translating results to the human system.

In humans, WM microstructure in healthy and pathological aging has been studied predominantly with DTI and related methods. Previous studies have established that age-related differences in WM mediate cognitive decline associated with aging, an association referred to as the “disconnection hypothesis” (Bennett & Madden, 2014). Because WM tracts differ in their susceptibility to aging, two main spatial gradients have been proposed to explain this selective vulnerability. First, the anterior-posterior gradient suggests that DTI-FA decreases in anterior brain regions relative to posterior regions (Bartzokis, 2004; Salat et al., 2005; Sullivan, Rohlfing, & Pfefferbaum, 2010b). For example, the effect of age tends to be greater in the anterior regions of the corpus callosum (Head et al., 2004). Second, the last-in-first-out hypothesis, also known as the retrogenesis hypothesis, assumes that WM regions that myelinate later in development deteriorate earlier with age (Bartzokis et al., 2010). For example, while decreases in FA are substantial in the late myelinating genu of the corpus callosum, regions such as the superior corona radiata show little evidence of decreased FA (Barrick, Charlton, Clark, & Markus, 2010; Burzynska et al., 2010).

DTI measures have also allowed researchers to make inferences about WM microstructure, including myelination of the human brain. In the normal development of the central nervous system, myelination occurs at a varied pace across the brain. Myelination begins

around the fourth month of embryonic development, increases rapidly in childhood and then its marked by successions of rapid growth and plateau phases that continue until the third or fourth decade of life, as confirmed by *post-mortem* and DTI studies (Kinney, Ann brody, Kloman, & Gilles, 1988; Kinney & Volpe, 2018; Lebel, Walker, Leemans, Phillips, & Beaulieu, 2008). Aligned with this, DTI studies have demonstrated nonlinear trajectories of FA and MD across the lifespan (Lebel et al., 2012). Because WM changes dynamically throughout the lifespan, even at older age (Engvig et al., 2012; Sampaio-Baptista & Johansen-Berg, 2017), we need to better understand the impact that WM and myelin plasticity have on cognitive function.

Cognitive aging refers to the effects of aging on all aspects of cognition (Salthouse, 1985). Age-related WM degeneration is thought to cause a “cortical disconnection” resulting in cognitive decline across several domains, particularly executive functions and processing speed (Sullivan, Rohlfing, & Pfefferbaum, 2010a). The processing-speed theory suggests that the main factor contributing to cognitive aging is a generalized slowing of performance that affects a variety of cognitive skills (Salthouse, 1996); in particular, age-related deterioration of the anterior WM is mostly associated with decreased verbal processing speed, while non-verbal processing speed is associated with deterioration of the superior longitudinal fasciculus, part of the fronto-parietal network. In addition, WM deterioration of other regions of the fronto-parietal network (e.g., prefrontal, anterior corpus callosum, superior/posterior parietal) has been associated with deficits in executive functions, such as inhibitory control and task-switching (Kennedy & Raz, 2009). Other authors suggest that decreased processing speed explains most of the age-related variance in executive composite scores (Albinet, Boucard, Bouquet, & Audiffren, 2012). All of these studies have used DTI parameters, but these are not specific to myelin or

axons. As a result, there are inconsistent associations of DTI and cognition (Rodrigue & Kennedy, 2011).

### **1.3. Lifestyle And White Matter Aging**

The cognitive trajectory associated with normal cognitive aging varies across individuals and is influenced by individual differences in biological, genetic, health, environmental and lifestyle factors. Lifestyle factors may attenuate the adverse effects of modifiable risk factors, such as vascular and metabolic conditions, and promote changes that can enhance cognition (Lindenberger, 2014). To be able to inform interventions on how to promote cognitive health, we have to consider the extent to which modifiable lifestyle factors can influence the course of WM aging. There is little doubt that lifestyle factors like physical activity provide extensive cardiovascular benefits, and that it can help reduce the burden of chronic diseases (Booth, Roberts, & Laye, 2012). Much less is known about the effects of physical activity on the progression of structural brain changes associated with cognitive aging, specifically, changes in WM.

Randomized controlled trials have shown that cardiorespiratory fitness can help reduce the detrimental effects of cognitive aging (Colcombe, Kramer, McAuley, Erickson, & Scalf, 2004). Cardiorespiratory fitness is defined as the maximum capacity of the cardiovascular and respiratory system to supply oxygen and deliver it to the body during sustained physical activity. Cardiorespiratory levels increase usually as a result of continuous aerobic exercise (Garber et al., 2011). Recent studies suggest that better cardiorespiratory fitness diminishes the adverse effects of cognitive aging (Voss et al., 2016). Indeed, there are only a few human intervention studies that have studied the effects of fitness training on human WM.

Physical activity and fitness training are effective methods to enhance brain plasticity (Hillman, Erickson, & Kramer, 2008); however, the effects of fitness training on the WM structure and cognition are inconsistent. Some of the variability in results can be attributed to variations in fitness levels (e.g., cardiorespiratory fitness levels, the intensity of daily physical activity), the heterogeneous methods used to measure physical activity, and the specific cognitive domains evaluated. Cross-sectional studies have shown that FA is positively correlated with fitness training, with higher FA values in the anterior corpus callosum, the superior corona radiata and the superior longitudinal fasciculus (Johnson, Kim, Clasey, Bailey, & Gold, 2012; Oberlin et al., 2016; Tseng et al., 2013). Most of these fascicles are late-myelinating, which suggests that late-myelinating regions may be more vulnerable to modifiable risk factors over and above effects of age (Wassenaar, Yaffe, van der Werf, & Sexton, 2019). Intervention studies have shown that exercise-induced increase in cardiorespiratory fitness correlated with FA change across the prefrontal and temporal WM (Voss et al., 2013). Still, little data exist on interventions that can prevent, slow or decrease WM deterioration.

Burzynska et al. (2017) provided the first evidence that declines in FA, RD, MD and axial diffusivity can be detectable on a short-term (6-month) scale in healthy older adults. In addition, this randomized controlled trial showed that 6-month exercise intervention resulted in a significant time-by-group interaction in the fornix, where dance group showed decrease in FA and increase in RD as compared to the control and walking groups, in which the FA declined and RD increased (Burzynska et al., 2017). A later randomized controlled study demonstrated short-term (6-month) changes in WM after dance-exercise intervention particularly in the corpus callosum and the superior longitudinal fasciculus (Rektorova et al., 2020). Together, these few findings suggest that WM of the adult brain demonstrates plasticity and these changes can be

observed on a short-term scale. Still, more randomized clinical trials are needed to understand the heterogeneity of effects that exercise-based interventions have on WM aging.

#### **1.4. Conventional MRI Methods**

Conventional MRI measures, including T1, T2, and T2\*, provide excellent tissue contrast and clinical sensitivity to macroscopic anatomical changes, like tumors or strokes. Therefore, T1-weighted images (T1-WIs) and T2-weighted images (T2-WIs) are commonly used to study brain structure and detect macroscopic abnormalities. A T1-WI or T2-WI can be collected in a relatively short time using standard MRI sequences, and such images are frequently acquired in multicenter studies, including the Alzheimer's Disease Neuroimaging Initiative (ADNI) (Jack et al., 2008). However, the biophysical processes that give rise to T1-WI and T2-WI contrast are not fully understood. Namely, same changes in image intensity may be caused by multiple histological processes, making T1- and T2-WIs not specific to any WM microstructural property (Deoni, 2010). Recently, the ratio of the signal intensities of T1-WIs and T2-WIs was proposed as a proxy for myelin content (Glasser & van Essen, 2011). Given the broad availability of T1-WIs and T2-WIs in the existing datasets, the T1w/T2w ratio offers an intriguing complementary measure of WM microstructure (Ganzetti, Wenderoth, & Mantini, 2014).

The different tissue contrasts in T1-WI and T2-WI arise largely from the differences in the T1 and T2 relaxation properties of tissues, leading to different biophysical properties (Sharma & Lagopoulos, 2010). The predominant contrast in a T1-WI is related to the time required for protons (hydrogen nuclei) to return to equilibrium magnetization (i.e. realign with the external magnetic field  $B_0$ ) after excitation by a radio-frequency pulse (known as T1-longitudinal relaxation). In contrast, T2 is limited by the de-phasing processes of the proton spins and interactions between them, known as T2-transverse decay. All mechanisms which contribute

to T1 contribute to T2, because returning to equilibrium magnetization also results in a loss of magnetization from the transverse plane (Deoni, 2010). For example, in WM the proton spins collide with macromolecules and myelin sheaths with hydrophobic properties, limiting water displacement, resulting in shorter T1 and T2 in WM as compared to the cell somas of the grey matter. This phenomenon underlies the good grey matter-WM contrast in T1- and T2-WIs. Because of the shorter T1 and T2 of WM, in T1-WI fat appears brighter than the gray matter, while in T2-WI fat appears darker than grey matter. In conventional T1-W and T2-W imaging, tissue contrast is created by optimizing the sensitivity of the signal to the differences in the relaxation times of these tissues (Deoni, 2010).

Since myelin increases signal in T1-WIs but decreases signal in T2-WIs, it has been proposed that the division of the T1-WI by the T2-WI can provide a new quantitative image (T1w/T2w ratio) that is more sensitive to myelin, a “myelin-enhanced contrast” (Glasser & van Essen, 2011; Harkins et al., 2016). However, simple division does not automatically cancel the different signal variations related to the different sensitivity profiles of the receiver coils of each image (Ganzetti, Wenderoth, & Mantini, 2016). The key requirement of any receiver coil is to obtain the maximum signal-to-noise ratio, so that the signal is stronger than the random variations in the intensity due to noise (Gruber, Froeling, Leiner, & Klomp, 2018). The variation in intensity in MRI is known as “intensity inhomogeneity” and needs to be corrected to obtain a standardized T1w/T2w contrast.

We can model the T1w/T2w contrast as

$$T1w/T2w \approx \frac{\alpha_1 * s_1 * x}{\alpha_2 * s_2 * \left(\frac{1}{x}\right)} = \frac{\alpha_1 * s_1}{\alpha_2 * s_2} x^2 = \beta x^2 \quad \text{EQ.2}$$

with the myelin contrast represented by  $x$  in the T1-WI and  $1/x$  in the T2-WI, the sensitivity of the receiver coils denoted by  $s1$  and  $s2$  for the T1-WI and T2-WI, respectively, and the  $\alpha1$  and  $\alpha2$  as scaling factors. Therefore, the T1w/T2w signal intensity depends on the combination of  $s1$ ,  $s2$ ,  $\alpha1$ , and  $\alpha2$  (Ganzetti et al., 2014). The idea of the intensity scaling procedure is to standardize  $\alpha1$  and  $\alpha2$ , so that the difference between the sensitivity profiles ( $s1$ ,  $s2$ ) of the T1-WI and T2-WI is negligible. By standardizing the images, the T1w/T2w can be comparable across subjects and may be a valid tool for non-invasive mapping of myelin in the brain that is not derived from the diffusion properties of the tissue.

To date, most studies using the T1w/T2w method have studied myelin content in the cortical gray matter, since the method was originally developed to create maps of human neocortex (Glasser & van Essen, 2011). However, myelin is distributed unevenly between the WM and the gray matter, with higher concentrations in the WM. Thus, the utility of the T1w/T2w to study WM properties still needs to be investigated. Some evidence has demonstrated that the T1w/T2w may be a valid tool to map intracortical myelin in the WM. For example, (Ganzetti et al., 2014) reported higher T1w/T2w values in WM structures where myelin is abundant, e.g., the posterior limb of the internal capsule and the corona radiata. Another study assessing intracortical myelin in the WM found an inverted U-shaped of the T1w/T2w ratio trajectory over the lifespan, particularly in the superior frontal, inferior parietal and temporal, and posterior cingulate cortices (Grydeland, Walhovd, Tamnes, Westlye, & Fjell, 2013). These results are aligned with studies describing a quadratic trajectory of myelination in the human

WM, with a maximum in mid-life (Bartzokis et al., 2010). Still, there are inconsistent associations between T1w/T2w ratios and quantitative myelin imaging methods such as myelin water fraction and magnetization transfer ratios (Nakamura, Chen, Ontaneda, Fox, & Trapp, 2017; Uddin, Figley, Marrie, & Figley, 2018). Even though the T1w/T2w may not be a specific measure of myelin, it is promising in providing complementary information to DTI. The availability of T1 and T2-WIs in the existing datasets warrants investigations on cognitive relevance of the T1w/T2w and its ability to detect age differences and within-person changes in WM.

### **1.5. Overview of the current study**

In this thesis, we aimed to compare T1w/T2w ratio to DTI metrics with respect to: 1) their utility to assess the effects of lifestyle interventions on WM; 2) the extent to which they correlate with cognition (processing speed); 3) their ability to detect short-term within-person change; 4) the extent to which they correlate with age; and 5) the extent to which they correlate with each other. We tested the following specific hypotheses:

- 1) If the T1w/T2w is more sensitive to myelin, we expect that the T1w/T2w will detect a greater number of significant time-by-intervention group interactions than DTI-FA. One region where we particularly expect to observe greater effect size is the prefrontal WM (Voss et al., 2013).
- 2) If the T1w/T2w is more specific to myelin, we expect that the whole WM T1w/T2w would be a better predictor of processing speed ability than FA. In addition, we also consider the fornix to be a predictor of processing speed ability as demonstrated in (Burzynska et al., 2017).
- 3) If the T1w/T2w is more specific to myelin than DTI-FA, and is not affected by crossing-fibers, the association between T1w/T2w and DTI metrics should be strongest in regions with

fiber orientational coherence—that is, where the diffusion tensor model is valid (e.g., midline of the corpus callosum)—as compared with regions with a similar level of myelin but a higher percentage of crossing fibers, such as crossing of corpus callosum and superior longitudinal fasciculus within the centrum semiovale. Furthermore, the associations between T1w/T2w and DTI-RD should be higher in regions that have higher myelin content (e.g., posterior limb of the internal capsule (Yagishita, Nakano, Oda, & Hirano, 1994)) when compared to regions with lower content of myelin (e.g. genu of the corpus callosum) (Lamantia & Rakic, 1990).

4) If the T1w/T2w is more specific to myelin, we expect this measure to capture the development to degeneration gradient; that is, to show greater negative associations with age in late-myelinating regions (e.g., genu and body of corpus callosum, fornix) as opposed to early-myelinated fiber tracts (e.g., superior corona radiata, posterior limb of the internal capsule).

## 2. CHAPTER 2: METHODS

### 2.1. Study Sample

The University of Illinois institutional review board approved this study, written informed consent was obtained from all participants and the study was performed in accordance with the 1964 Declaration of Helsinki. The sample was recruited to participate in a randomized controlled exercise trial (Fit & Active Seniors Trial at ClinicalTrials.gov, clinical study identifier NCT01472744). Healthy, low active older adults were recruited in the Champaign county area to participate in a series of neuroimaging, cognitive, and cardiorespiratory testing, before and after a 6-months aerobic exercise intervention program. Of the 1,119 participants recruited, 247 (n = 169 women) met inclusion criteria and agreed to enroll in the study. Eligible participants met the following criteria: (1) were between the ages of 60 and 80 years old; (2) were free from psychiatric and neurological illness and had no history of stroke or transient ischemic attack; (3) scored <10 on the geriatric depression scale (GDS-15); (4) scored  $\geq 75\%$  right-handedness on the Edinburgh Handedness Questionnaire; (5) demonstrated normal or corrected-to-normal vision of at least 20/40 and no color blindness; (6) cleared for suitability in the MRI environment; that is, no metallic implants that could interfere with the magnetic field or cause injury, no claustrophobia, and no history of head trauma; (7) reported to have participated in no more than two moderate bouts of exercise per week within the past 6-months; (8) were not taking medication for cardiovascular disease (e.g., beta blocker, diuretics), neurological, or psychiatric conditions (e.g., antidepressant, neuroleptic, anxiolytic). We included a subset of 174 participants who had good quality pre and post-intervention diffusion scans and excluded 5 participants that did not have sufficient brain coverage to perform T2-WI preprocessing for

T1/T2 ratio; the final sample consisted of 169 participants and all of them scored  $\geq 26$  on MMSE suggesting normal cognitive status.

Perceptual speed was measured with a linear combination of measures obtained via PCA from the Virginia Cognitive Aging Battery (Salthouse et al., 2016), as described earlier in (Burzynska et al., 2017). The tasks that had high loadings on perceptual speed construct were: letter comparison, pattern comparison, and digit symbol substitution.

## **2.2. Intervention**

Participants were enrolled into a six-month intervention program which consisted of four conditions (aerobic, aerobic + nutrition, dance, and control). All conditions were controlled and monitored, as previously described (Burzynska et al., 2017). The walking/aerobic condition consisted of an exercise program of brisk walking. Heart rate was monitored frequently using palpation and heart rate monitors. The walking/aerobic + nutrition condition consisted of an exercise program of brisk walking accompanied by regular administration of a dietary supplement. The dietary supplement contained beta-alanine, an amino acid that increases physical performance and promotes muscle growth. The stretching and toning control condition consisted of structured sessions of stretching, toning, and balance specially designed for older individuals. The active control condition was designed to not result in significant increases in cardiorespiratory fitness (Colcombe et al., 2004). Finally, the dance condition consisted of a combination of dance types including ballroom, Latin square-dancing, polka, line-dancing, swing, and folk.

### **2.3. MRI Acquisition**

We acquired all images during a single session on a 3T Siemens Trio Tim system with 45 mT/m gradients and 200 T/m/sec slew rates (Siemens, Erlangen, Germany). Structural MR scans were acquired using a 3D MPRAGE T1-w sequence (TR = 1900 ms; TE = 2.32 ms; TI: 900 ms; flip angle = 9°; matrix = 256 × 256; FOV = 230mm; 192 slices; resolution = 0.9 × 0.9 × 0.9 mm; GRAPPA acceleration factor 2).

Diffusion-weighted images (DWI) were obtained parallel to the anterior-posterior commissure plane with no interslice gap. DWI were acquired with a twice-refocused spin echo single-shot Echo Planar Imaging sequence (Reese et al., 2003) to minimize eddy current-induced image distortions. The protocol consisted of a set of 30 non-collinear diffusion-weighted acquisitions with b-value = 1,000 s/mm<sup>2</sup> and two T2-w b-value = 0 s/mm<sup>2</sup> acquisitions, repeated two times (TR/TE = 5,500/98 ms, 128 × 128 matrix, 1.7 × 1.7 mm<sup>2</sup> in-plane resolution, FA = 90, GRAPPA acceleration factor 2, and bandwidth of 1698 Hz/Px, comprising 40 3-mm-thick slices).

### **2.4. MRI Preprocessing**

DTI data were processed using the FSL 4.1 Diffusion Toolbox (FDT: <http://www.fmrib.ox.ac.uk/fsl/>, a part of FSL (Smith 2004) in a standard multistep procedure, including: 1) motion and eddy current correction using the “eddy\_correct” tool; 2) removal of the skull and non-brain tissue using the Brain Extraction Tool (Smith, 2002); and 3) voxel-by-voxel calculation of the diffusion tensor using DTIFIT (Behrens et al., 2003). Additionally, RD was calculated as the mean of the second and third eigenvalues (Burzynska et al., 2010; Song et al., 2002).

Group analyses require co-registration of diffusion images to a standard template. However, standard registration algorithms are not a satisfactory solution to the problem of aligning FA images from multiple subjects without making biased assessments of localized changes in the major WM tracts. Also, due to increased anatomical heterogeneity in older populations (i.e. different degrees of atrophy and ventricular enlargement), standard registration algorithms are often not optimal. Therefore, we decided to use TBSS (Tract-Based Spatial Statistics), which uses a nonlinear registration tool to align images into a common space by using a b-spline representation of the registration warp field (Rueckert, 1999; Smith et al., 2006). This b-spline representation allows to estimate the amount of similarity between the warped image and fixed image and optimizes the registration. Moreover, TBSS then estimates a “group mean FA skeleton” representing the center of the WM tract. Skeletonization and projection of center-of-tract values allows to focus the analyses on the local center of tracts, avoiding regions with too much variability produced by inter-subject anatomy, as well as WM lesions or partial volume with grey matter or CSF. Finally, the TBSS process minimizes the amount of warping/smoothing required for alignment of the DTI images to the standard template.

After creating the FA images, TBSS applies nonlinear registration of all FA images into a 1x1x1mm standard Montreal Neurological Institute (MNI152) space via the FMRIB58\_FA template using the FMRIB's Nonlinear Registration Tool (FNIRT, Rueckert et al., 1999). Then, it creates the mean FA image of the sample. Next, the WM “skeleton” is created by perpendicular non-maximum-suppression of the mean FA image and setting the FA threshold to 0.25. Lastly, using a perpendicular search restricted by a “distance map” the highest FA values (local center of the tract) were projected onto the skeleton, separately for each subject. The same procedure was repeated for RD and T1w/T2w using non-FA pipeline.

## 2.5. T1w/T2w Ratio Calculation

We used our MPRAGE T1-weighted images and the T2-weighted  $b=0\text{s/mm}^2$  images from the DWI acquisition to calculate the T1w/T2w ratio. We used the T2-WIs  $b_0$  images from the DWI since our MRI protocol did not include T2-WIs (we had FLAIR, but CSF suppression causes hypo-attenuation of grey matter which leads to a decrease in grey-WM contrast). To generate the T1w/T2w ratio we used a preprocessing workflow developed to generate an optimized contrast technique (Ganzetti et al., 2014), using the MRTool registration-segmentation framework in SPM12 (Wellcome Trust Centre for Neuroimaging, London, UK). Initially, original T2-WIs in the individual space were co-registered to T1-WIs through a rigid-body transformation using SPM tools. Because the raw T1-WIs and T2-WIs are not quantitative and their signal intensities vary among different scanners and scan sessions, the images need to be bias-corrected to ensure that the sensitivity profiles are equal and, therefore, comparable across subjects. The input parameters for the bias correction algorithm, including the smoothing and the regularization parameters, were set at their default values (60 mm and  $10^{-4}$ ). The regularization parameter sharpens intensity transitions between image structures, whereas the bias field smoothing models the smoothness of the intensity inhomogeneity. After bias correction, the images were processed to standardize their intensity scales, a step known as calibration (Ganzetti et al., 2014). We decided to use a non-linear internal image calibration, that chooses an internal hallmark inside the brain to standardize the intensity values. We did not apply the recommended external calibration (using tissue outside the brain such as the eye or neck muscle) since some of the T2-WIs did not have full brain coverage. After image calibration, T1w/T2w ratios were calculated to generate the final T1w/T2w images. Figure 1 summarizes the preprocessing pipeline for the

T1w/T2w ratio. Finally, each subject's T1w/T2w images in MNI space were entered into the TBSS non-FA procedure after the registration step, and projected onto the FA skeleton.

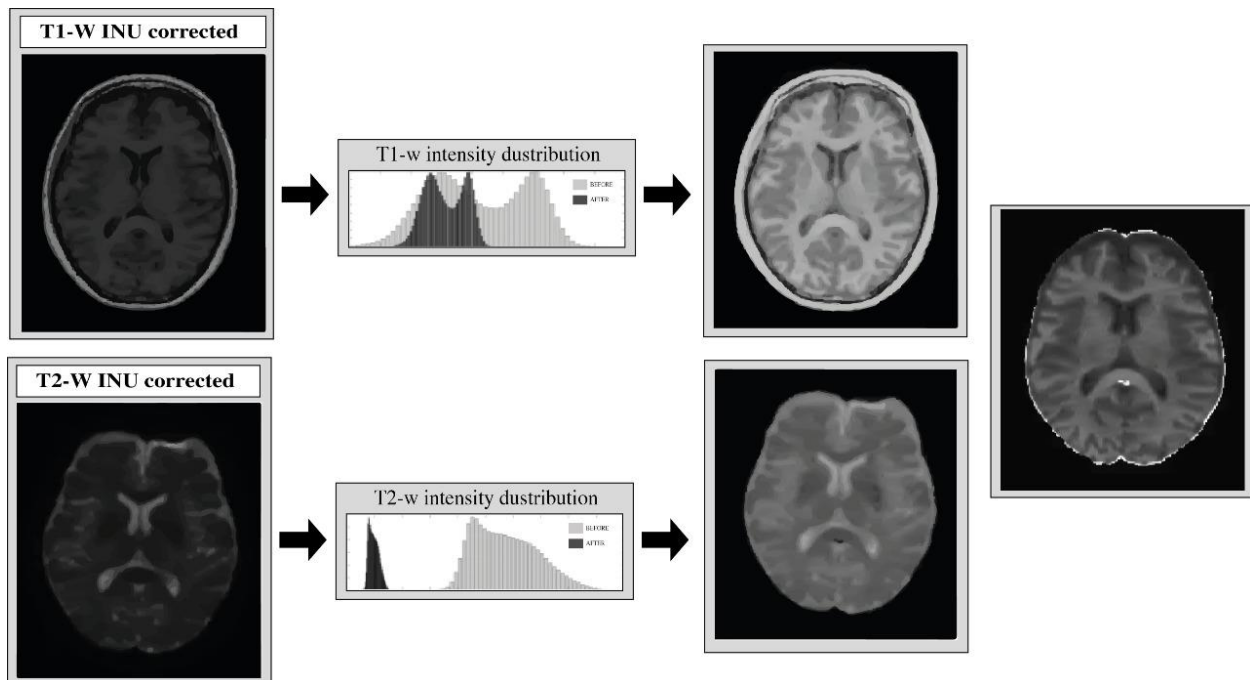


*Figure 1.* Calculation of the calibrated T1w/T2w ratios. After the T2-WIs were co-registered to the T1-WIs, the images were entered into the bias correction algorithm. From left to right: T1 and T2-WIs after adjusting for intensity inhomogeneity, T1 and T2-WIs after calibration, T1w/T2w ratio image in MNI space. Modified from: “*Whole brain myelin mapping using T1- and T2-weighted MR imaging data*”, by M. Ganzetti, 2014, *Frontiers in Human Neuroscience*, pp. 671. Copyright by Frontiers in Human Neuroscience.

## 2.6. Regions-Of-Interest

To obtain the FA, RD and T1w/T2w from the total WM, for each participant, we extracted a mean of all voxels projected onto the skeleton. In addition, we extracted mean values for the following 12 regions of interest (ROIs) in the WM: superior corona radiata (SCR), superior longitudinal fasciculus (SLF), anterior and posterior limb of the internal capsule (ALIC and PLIC), external capsule (EC), fornix (FX), 5 regions of the corpus callosum [reg1, 2, 3, 4, 5], WM of the medial prefrontal cortex (prefrontal WM).

Each ROI was manually defined on the TBSS skeleton overlaid on mean FA image using the DTI-WM atlas, as described in (Burzynska et al., 2013; Oishi, Faria, & van Zijl, 2012). The WM atlas we used was normalized to the ICBM-152 brain in MNI coordinates (Oishi et al., 2012). Figure 2 shows the 12 WM ROIs.

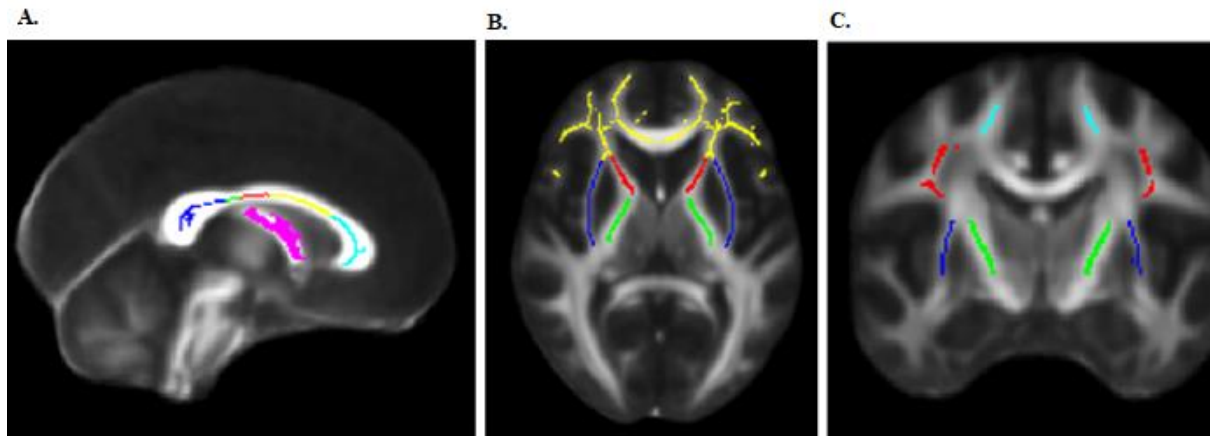


*Figure 2.* Regions of interest. A: reg1cc in light blue, reg2cc in yellow, reg3cc in green, reg5cc in blue and the FX in fuchsia. B: prefrontal WM ROI in yellow, the ALIC in red, EC in blue and the PLIC in green. C: the SCR in light blue, the SLF in red, the EC in blue and the PLIC in green.

To study the anterior-posterior gradient of WM degeneration (Head et al., 2004), we extracted five segments along the anterior-posterior length of the CC using the scheme established by DTI-based tractography (Hofer & Frahm, 2006). Region 1 (reg1cc) contains the most anterior fibers of the CC, which project to the prefrontal cortex. Region 2 (reg2cc) projects to the premotor and supplementary control areas. Region 3 (reg3cc), the posterior mid-body projects to the primary motor cortex. Region 4 (reg4cc) projects to the primary sensory cortex. The most posterior region (reg5cc), where callosal parietal, temporal and occipital fibers cross the CC is region 5. Because the distinct sub-regions of the CC are not homogeneous and they reveal wide diversity of fiber calibers and axonal composition, we selected larger highly myelinated fibers (reg3cc and reg4cc) and densely packed but lightly myelinated thin fibers

(reg1cc) to compare high vs. low myelin content WM regions (Lamantia & Rakic, 1990; Vincze, Mázló, Seress, Komoly, & Ábrahám, 2008).

To study the retrogenesis hypothesis (Brickman et al., 2012; Reisberg et al., 1999), we included the PLIC and the SCR as the early-myelinated WM regions. For the late-myelinated regions, we selected three regions that myelinate ~68 weeks after birth (reg3cc, reg4cc, reg5cc), two regions that myelinate ~70-109 weeks after birth, EC and reg1cc. Lastly, we selected one region that myelinates >144 weeks after birth, FX; (Kinney & Volpe, 2018; Slater et al., 2019). From these ROIs, we selected one region with higher myelin content, the PLIC, as confirmed by post-mortem studies (Yagishita et al., 1994). We included the FX as a lower myelin content region since it contains small-diameter fibers with thin myelin sheaths and about 40% unmyelinated nerve fibers (Peters, Sethares, & Moss, 2010). In addition, we included the ALIC, since the highest T1w/T2w values have been reported on this region (Ganzetti et al., 2014).

Because of the important implications in cognitive aging and vulnerability to lifestyle interventions (Gunning-Dixon, Brickman, Cheng, & Alexopoulos, 2009; Tseng et al., 2013), we included a prefrontal WM ROI and the SLF. Finally, we selected two reference points: two crossing fiber regions and two grey matter regions. We manually defined two fiber crossing regions at the crossing of commissural (the corpus callosum), association (SLF) and projection fibers (the corticospinal tract) and created two masks located in the following MNI coordinates: -11, 24, 37 (left anterior centrum semiovale) and -27, -7, 30 (middle centrum semiovale). A similar approach to extract high-crossing fiber regions was described in (Jeurissen, Leemans, Jones, Tournier, & Sijbers, 2011). Because myelin is distributed unevenly between the WM and the gray matter, with higher concentrations in the WM, we selected two grey matter regions in

the subcortical grey matter (caudate, thalamus), using the Harvard-Oxford subcortical anatomical atlas.

## **2.7. Statistical Analyses**

To study intervention effects, we first used repeated measures ANOVA to investigate the effects of time (pre vs. post-test) and the effect of the intervention by looking at the interaction between time vs. treatment groups (control, dance, aerobic, and aerobic + nutrition). We replicated previous results that used DTI-FA and then we analyzed the T1w/T2w.

To address hypothesis 1, we decided to group our intervention groups into a binary variable (i.e., aerobic exercise vs. control), because prior results suggest that all active intervention groups show similar outcomes (Burzynska et al., 2014, 2017). Then, to compare control vs. intervention groups over time we used linear mixed-effects models fitted to the data using the R lme4 package. Models included fixed effects for time, group, and the time-by-group interaction. The model also included a random intercept. Time and group were dummy coded, where control=0 and intervention group=1.

To address hypothesis 2, we used multiple linear regression models, we regressed processing speed onto WM predictors controlling for age and education. Model 1 included age and education. Model 2 added total T1w/T2w and FA WM values. Because DTI-FA has previously been associated with decreased processing speed in the fornix (Burzynska et al., 2017) we also looked at the T1w/T2w fornix in Model 3. To ensure that our intercept (the predicted value for processing speed) represented the corrected mean (predicted value for processing speed, holding covariates at their mean values), we standardized our variables by subtracting the mean of the variable and dividing by the variable's standard deviation (SD).

Standardized regression coefficients represented the expected change in processing speed's SD for a 1-SD increase in each of the predictors. For model comparisons, we examined change in  $R^2$  ( $\Delta R^2$ ).

To address hypothesis 3, we studied the association of the T1w/T2w and DTI metrics using linear mixed-effects models. The hypothesis (moderator hypothesis) was that the association between T1w/T2w and DTI metrics depended on ROI. Thus, we regressed DTI values onto fixed effects of brain region, T1w/T2w, and the brain region-by-T1w/T2w interaction. Models also included a random intercept. For this, we focused on the region-by-T1w/T2w interaction. We looked at two brain regions at the time by incorporating "brain area" as a binary variable. Area is a binary variable that was dummy coded to contrast the difference between ROIs (e.g., PLIC=0, reg1cc=1). We ran 12 linear mixed-effects models in total. For our models, we standardized all quantitative variables, but not factors, to create partially standardized regression coefficients. The standardization of our variables rendered regression coefficients ( $\beta$ ) interpretable in the correlation-like metric.

Finally, to test hypothesis 4, we estimated Pearson's correlations to examine the associations between T1w/T2w and age and between FA and age in selected ROIs. For the size of our correlations and effects, we used (Cohen, 1992) recommendations, where a correlation of 0.50 is a large-sized effect, 0.30 is a medium-sized effect and 0.10 is a small-sized effect. Lastly, to visually compare the different kinds of images (T1w/T2w vs. FA), we calculated the average and SD for the intensity values for each ROI; for this we selected the two grey matter regions (caudate nucleus and thalamus), four WM regions (SCR, PLIC, ALIC, reg1cc) and two crossing fiber regions (anterior and medial centrum semiovale).

### 3. CHAPTER 3: RESULTS.

First, Pearson correlations for the FA values between our sample (n =169) and the original sample (n =174, Burzynska et al., 2017) were all above 0.9, indicating that the exclusion of 5 participants and reanalysis of the TBSS procedure did not meaningfully affect data consistency (Appendix A).

#### Baseline characteristics

We tested whether randomization based on age and sex resulted in same baseline characteristics among the control and intervention groups. Table 1 shows the baseline characteristics for the final sample of 169 participants. One-way ANOVA revealed that the two groups did not differ with respect to age, gender, education years and general health variables.

Table 1. Baseline characteristics of the sample

<b>Variables</b>	<b>Control n=40</b>	<b>Intervention group n=129</b>	<b><i>p</i> value</b>
Age	66.2±4.6	65.1±4.3	0.178
Women, n (%)	27 (67.5)	90 (69.8)	0.845
Education, yrs	16.2±3.0	15.7±2.9	0.378
MMSE	28.4±1.3	28.5±1.4	0.937
BMI	30.7±6.2	30.4±5.3	0.776
Systolic BP	131.7±14.6	132.2±13.5	0.841
Diastolic BP	79.4±8.0	79.4±8.0	0.999
Resting HR	73.1±9.7	73.2±10.4	0.942
Average MVPA	44.9±28.5	42.6±24.6	0.634
VO <sub>2</sub> Max	19.4±4.2	19.9±4.3	0.533
Total T1w/T2w	1.40±0.03	1.40±0.02	0.765
Total FA	0.46±0.01	0.46±0.02	0.620

Note: MMSE= Mini-mental state examination, BMI= body mass index, BP=blood pressure, HR=heart rate, MVPA= moderate to vigorous physical activity. Quantitative data is presented as mean and standard deviation (±) and qualitative data as frequencies and percentages. *p* value of the comparison of the baseline information between control vs. intervention group.

### 3.1. Intervention Effects

Using linear mixed-effects models, we analyzed changes in T1w/T2w and FA over 6-months, focusing on the evaluation of the time-by-intervention group interaction effect. We used  $\beta$  coefficients to represent the standardized effects of the average of the control group vs. the intervention group (Figure 3).

We found significant time-by-intervention interaction effects for the T1w/T2w in the following WM regions: reg1cc ( $\beta=0.25$ ,  $p=0.014$ ,  $SE=0.09$ ), reg5cc ( $\beta=0.17$ ,  $p=0.003$ ,  $SE=0.05$ ), PLIC, ( $\beta=0.27$ ,  $p=0.002$ ,  $SE=0.08$ ), ALIC, ( $\beta=0.33$ ,  $p=0.001$ ,  $SE=0.09$ ) and prefrontal WM ( $\beta=0.22$ ,  $p=0.043$ ,  $SE=0.10$ ). For FA, the interaction was significant only in the fornix ( $\beta=0.08$ ,  $p=0.015$ ,  $SE=0.03$ ). All other coefficients are reported in Appendix B.

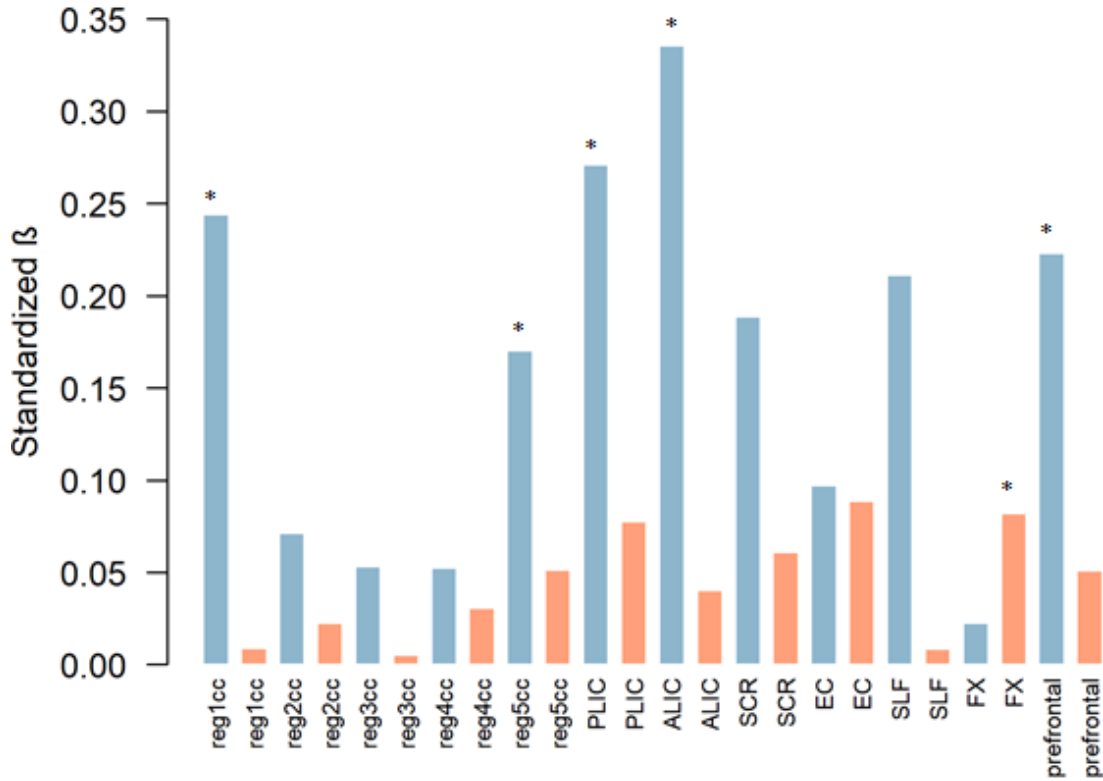


Figure 3. Standardized  $\beta$  coefficients displaying the effect size of the time-by-intervention group interaction. Blue = T1w/T2w. Orange = FA. Asterisks indicate

significant effects. CC =corpus callosum, PLIC =posterior limb of the internal capsule, ALIC =anterior limb of the internal capsule, SCR =superior corona radiata, EC =external capsule, SLF =superior longitudinal fasciculus, FX =fornix.

## **ANOVA results**

Using repeated measures ANOVA, we also replicated results from Burzynska et al (2017), showing significant time-by-group interactions only in the fornix (Appendix C).

### **3.2. Associations with Processing Speed**

Processing speed was regressed on age and education; subsequent models added predictors to study their impact and significance within the model. Multiple linear regression models showed that the T1w/T2w in the whole-WM, age and education were significant predictors of processing speed (Table 2). In Model 2 we observed that for a 1-*SD* increase in age, processing speed decreased by 0.41 *SD* ( $p < 0.001$ ), for a 1-*SD* increase in education, processing speed increased by 0.17 ( $p = 0.02$ ) and for a 1-*SD* increase in the T1w/T2w processing speed decreased by 0.13 ( $p = 0.02$ ), while FA was not significant at trend level. In Model 3, only age and education were significant predictors of processing speed; the T1w/T2w in the FX was not significant.

Table 2. Multiple linear regression analysis with processing speed as the dependent variable.

Model 1					Model 2					Model 3				
IV	$R^2$	$\beta$	SE	$p$ -value	$R^2$	IV	$\beta$	SE	$p$ -value	$R^2$	IV	$\beta$	SE	$p$ -value
Age	0.15	-0.36	0.072	<b>0.01</b>	0.19	Age	-0.41	0.076	<b>0.01</b>	0.16	Age	-0.33	0.074	<b>0.01</b>
Edu		0.13	0.072	<b>0.07</b>		Edu	0.17	0.073	<b>0.02</b>		Edu	0.13	0.072	0.07
						Total FA	-0.16	0.072	0.08		T1w/T2w FX	0.08	0.074	0.29
						Total T1w/T2w	-0.13	0.075	<b>0.02</b>					

Note: IV: independent variables, SE= standard errors, Edu=education. Change in  $R^2$  values model 1 vs. model 2 =  $\Delta R^2 = .195 - .157 = 0.038$ . Model 1 vs. model 3,  $\Delta R^2 = 0.165 - 0.157 = 0.008$ .

### 3.3. Associations Between DTI and T1w/T2w

Using linear mixed-effects models, our goal was to determine whether the association between the T1w/T2w and DTI metrics depended on ROI. For this, our focus was on the region-by-T1w/T2w interaction. Table 3 shows the associations between T1w/T2w and FA at baseline in regions with high vs. low myelin content, and regions with high vs. low fiber coherence.

We found positive associations between FA and the T1w/T2w in the FX ( $\beta = 0.56$ ,  $p = 0.0001$ ) and in the reg1cc ( $\beta = 0.37$ ,  $p = 0.001$ ), when compared to the PLIC. FA and the T1w/T2w had a significant positive association in reg1cc when compared to the ALIC. There was less association between FA and the T1w/T2w in regions with low fiber coherence (anterior and middle centrum semiovale), when compared to a region with high fiber coherence (reg1cc).

Table 3. Associations between FA and T1w/T2w by ROI

<i>Fixed effect for the interaction term (T1w/T2 by area)</i>			
	$\beta$	<i>p</i> value	Std. Error
<b>Higher vs. lower myelin content regions</b>			
<b>PLIC vs. FX</b>			
T1/T2-by-area	0.56	<b>0.001</b>	0.075
<b>PLIC vs. reg1cc</b>			
T1/T2-by-area	0.37	<b>0.001</b>	0.11
<b>reg3cc vs. reg1cc</b>			
T1/T2-by-area	0.28	0.104	0.17
<b>reg4cc vs. reg1cc</b>			
T1/T2-by-area	0.19	0.319	0.19
<b>ALIC vs. reg1cc</b>			
T1/T2-by-area	0.148	<b>0.001</b>	0.04
<b>High vs. Low fiber coherence region</b>			
<b>reg1cc vs. middle CS</b>			
T1/T2-by-area	-0.11	<b>0.001</b>	0.02
<b>reg1cc vs. anterior CS</b>			
T1/T2-by-area	-0.054	<b>0.004</b>	0.01

Note: CS= centrum semiovale.

Similarly, we also studied the associations between the T1w/T2w and RD. We decided to compare these associations in regions with high vs. low myelin content. Contrary to FA, we observed that there was a negative association between RD and T1w/T2w in the FX ( $\beta = -0.95$ ,  $p = 0.001$ ) and in the reg1cc ( $\beta = -0.35$ ,  $p = 0.001$ ) when compared to the PLIC (a higher myelin content region). Similarly, the association between RD and T1w/T2w was smaller for the reg1cc when compared to the reg3cc and ALIC (Table 4), implying that there are more associations between RD and the T1w/T2w among regions with higher myelin content.

Table 4. Associations between RD and T1w/T2w by ROI

*Fixed effect for the interaction term (T1w/T2w by area)*

	$\beta$	p value	Std.Error
<b>Higher vs. lower myelin content regions</b>			
<b>PLIC vs. FX</b>			
T1/T2-by-area	-0.95*	<b>0.001</b>	0.10
<b>PLIC vs. reg1cc</b>			
T1/T2-by-area	-0.35	<b>0.001</b>	0.08
<b>reg3cc vs. reg1cc</b>			
T1/T2-by-area	-0.35	<b>0.025</b>	0.15
<b>reg4cc vs. reg1cc</b>			
T1/T2-by-area	-0.15	0.368	0.17
<b>ALIC vs. reg1cc</b>			
T1/T2-by-area	-0.28	<b>0.001</b>	0.08

\*The parameter estimate from this model should be interpreted carefully because of model non-convergence (singularity).

### 3.4. Correlations with Age

We found that the T1w/T2w was negatively correlated with age in the FX and middle regions of corpus callosum (cc2,3,4) and positively correlated with age in the PLIC and EC (Table 5). For FA, we observed negative correlations with age in the whole WM, the most anterior regions of the corpus callosum, the SCR, the FX and the prefrontal WM. The anterior-

to-posterior gradient of correlations with age (Lamantia & Rakic, 1990; Sullivan, Rohlfing, et al., 2010b), for FA and T1/T2 is represented in Figure 4.

**Table 5. Correlations of T1w/T2w and FA with age**

	whole WM	reg1 cc	reg2c c	reg3c c	reg4 cc	reg5 cc	PLIC	SCR	EC	SLF	FX	prefrontal
<b>T1w/T2w</b>												
$\rho$	-0.06	0.03	0.29*	0.25*	0.22*	-0.1	0.17*	-0.1	0.18*	0.03	0.27*	-0.07
<b>FA</b>												
$\rho$	-0.361	0.23*	0.18*	-0.15	0.12	0.07	0.05	0.34*	0.23*	0.21*	0.36*	0.40**

Note:  $\rho$  = Pearson's correlation coefficient. \*  $p$  value <0.05. \*\*  $p$  value <0.01. CC=corpus callosum, PLIC=posterior limb of the internal capsule, ALIC=anterior limb of the internal capsule, SCR=superior corona radiata, EC=external capsule, SLF=superior longitudinal fasciculus, FX=fornix

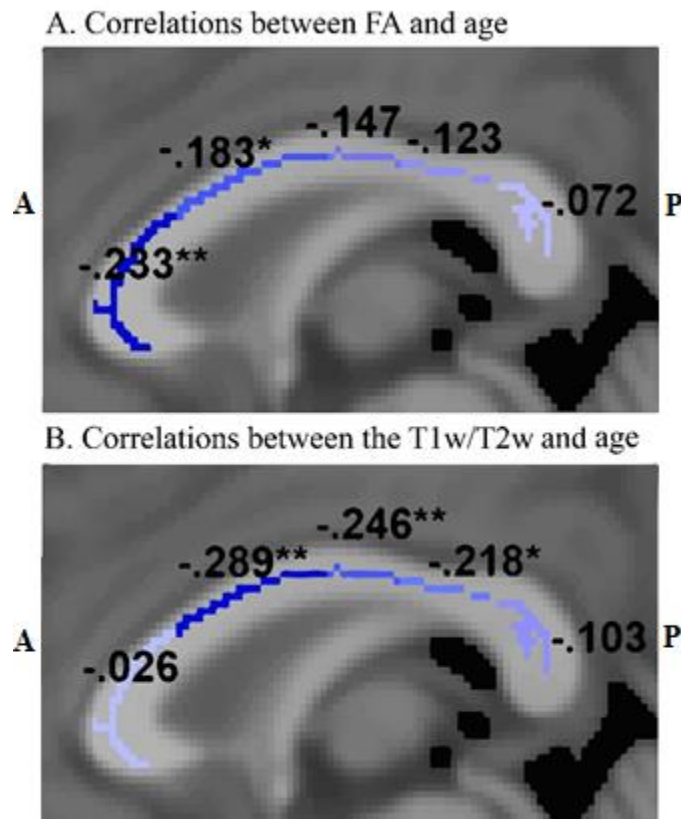


**Figure 4.** A heat map of Pearson's correlations in the corpus callosum. Dark blue indicates strong, negative correlations and light blue indicates weak, negative correlations. A=anterior; P=posterior. Asterisks indicate significant results from the correlations. \* $p$  value <0.05. \*\* $p$  value <0.01.

### 3.5. T1w/T2w and FA values in White Matter vs Grey Matter

We selected two grey matter regions (caudate nucleus and thalamus), four WM regions (SCR, ALIC, PLIC and reg1cc) that have high T1w/T2w values (Ganzetti et al., 2014) and two high crossing-fiber regions (anterior and middle centrum semiovale). The grey matter ROIs had lower T1w/T2w values than all WM regions (Figure 5), while crossing-fiber WM regions had similar values as the non-crossing WM ROIs. For FA, we observed that the grey matter ROIs and the crossing fiber regions had lower FA values than all WM regions (Figure 6).

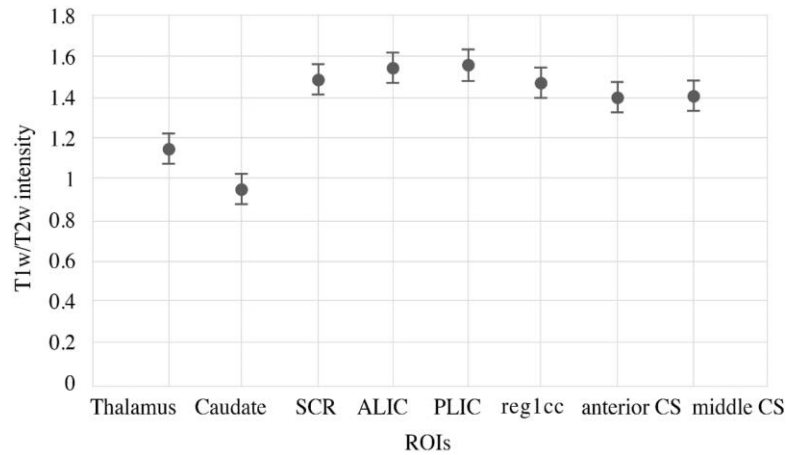


Figure 5. T1w/T2w intensity values in WM and grey matter regions. Figure shows the mean and SD of the T1w/T2w in selected ROIs.

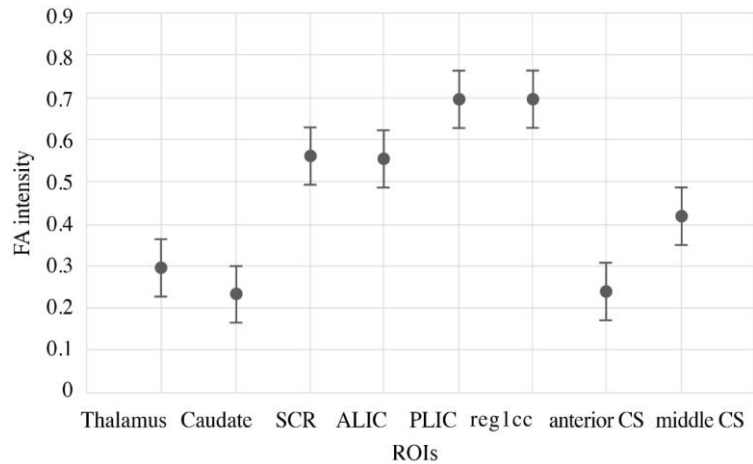


Figure 6. FA intensity values in WM and grey matter regions. Figure shows the mean and SD of FA in selected ROIs.

## 4. CHAPTER 4: DISCUSSION

The present study explored the associations between the T1w/T2w ratio and DTI metrics with respect to their ability to study the effects of lifestyle interventions in WM microstructure, their ability to predict decreased processing speed ability and their correlations with age and each other. This study's main findings were: 1) T1w/T2w produced a greater number of significant time-by-intervention group interactions than DTI-FA 2) whole WM T1w/T2w correlated with processing speed, controlling for age and education; 3) T1w/T2w was more strongly associated with DTI in regions with higher fiber orientational coherence and higher myelin content when compared with regions with low myelin content and low fiber coherence; and 4) T1w/T2w was associated with age, in particular in regions with high myelin content.

In this section I review the main findings in the context of the existing literature, discuss potential biological mechanisms linking lifestyle interventions and WM plasticity, consider implications of the findings with respect to future research and discuss methodological considerations.

### **4. 1. White matter and myelin plasticity**

Although aging WM is vulnerable to myelin loss and pathological degeneration, lifestyle factors, such as exercise, can enhance myelin plasticity during adulthood (Sampaio-Baptista & Johansen-Berg, 2017). Animal studies have demonstrated that aerobic exercise training results in greater degree of fiber myelination, greater number of myelinated axons and increased axonal diameter of myelinated axons (Bobinski et al., 2011; Chen et al., 2019). Particularly, oligodendrocyte dynamics appear to be regulated by experience; e.g., physical activity has been

found to increase the differentiation of oligodendrocytes progenitors into mature oligodendrocytes (Simon, Götz, & Dimou, 2011).

#### **4.2. Molecular pathways linking exercise and WM integrity**

In animal models, neurogenesis induced by aerobic exercise has been proposed to be caused by the secretion of growth factors. Examples include brain derived neurotrophic factor, which is known to activate molecular pathways crucial for spinogenesis, axonal regeneration and synaptic transmission (Chen et al., 2019), and insulin-like growth factor, which has been found in elevated levels in the prefrontal cortex of exercised rats (Uysal et al., 2017), and have been shown to enhance myelination in aged rats (Hlavica et al., 2017). Another proposed mechanism for increased WM integrity with exercise is a reduction in arterial stiffness, which has been demonstrated in old mice (Fleenor, Marshall, Durrant, Lesniewski, & Seals, 2010), and which ameliorates WM injuries of vascular origin (Lee et al., 2017).

In humans, other molecular mechanisms linking exercise and WM integrity have been proposed. Aerobic exercise attenuates the effects of vascular oxidative stress and inflammation through various mechanisms, including by reducing the expression of reactive oxygen species, decreasing endothelial dysfunction and reducing pro-inflammatory markers of chronic systemic inflammation (Craighead, Freeberg, & Seals, 2019; Lavin et al., 2020). Thus, aerobic exercise interventions could improve vascular function and provide anti-inflammatory effects, attenuating the effects of vascular insufficiency and inflammation on the brain's WM.

#### **4.3. In-vivo WM imaging and intervention effects**

We observed greater effect sizes for the time-by-intervention interaction in most WM regions using the T1w/T2w metric than using DTI-FA. The highest effect sizes observed were in

the PLIC and ALIC, which are highly myelinated regions (Chopra et al., 2018; Yagishita et al., 1994). These “high-myelin content” regions had the highest T1w/T2w intensity values, consistent with previous work in (Ganzetti et al., 2014). In addition, our findings suggest that exercise lifestyle interventions aid in the preservation of the structure of WM and that the T1w/T2w is capable of detecting intervention effects.

However, it is unclear whether the intervention effects that we see are due to changes in myelin content or vascular changes in the WM. The PLIC is an early-myelinating region and is also susceptible to the effects of arterial stiffness, cerebral hypoperfusion and hypoxic/ischemic events (Moody, Bell, & Challa, 1990). Cardiovascular risk factors such as hypertension are associated with increased small vessel strokes, mainly in the internal capsule (Shi & Wardlaw, 2016), suggesting that the PLIC is a region vulnerable to microvascular damage. In addition, cardiorespiratory fitness reduces arterial stiffness (Albin, Brellenthin, Lang, Meyer, & Lee, 2020), but it remains unknown whether this effect extends to the cerebral microcirculation in older adults. To our knowledge, only one study has proved that greater cerebral arterial stiffness is associated with increased WM lesions in normal aging (Tan et al., 2019), which would lead to a non-myelin-associated T1w/T2w signal. Therefore, some of our signal may be due to this effect rather than being a pure myelin signal.

The ALIC is another high myelin content region where we observed significant intervention effects. Since the ALIC contains axonal projections from the thalamic nuclei to the prefrontal cortex, it is possible that aerobic exercise counteracts the accelerated injury observed in the prefrontal WM and that the effect of aerobic exercise-intervention is consistently significant in regions that directly connect with the prefrontal cortex (e.g., ALIC, reg1cc). In one of the first randomized clinical trials studying aerobic fitness, fifty-nine sedentary community-

dwelling adults (aged 60-79 years) participated in an aerobic fitness intervention (Colcombe et al., 2006), and the greatest advantage of the intervention was observed in the ALIC. However, in this study they only included T1-WIs, which uniquely allows to study the WM macrostructure.

Still significant, but smaller effect sizes were seen in the reg1cc and prefrontal WM, which are late-myelinating regions and are known to be susceptible to aging and intervention effects (Voss et al., 2013). In their study among community-dwelling older adults (mean age=64.8), Voss and colleagues demonstrated that the aerobic exercise intervention affected mean FA across different brain regions, with the greatest effect observed in the prefrontal FA. Nevertheless, the effect sizes observed in (Burzynska et al., 2017; Voss et al., 2013) for the time-by-intervention effects were generally small. In the current study we observed that the T1w/T2w had greater effect sizes than FA to detect time-by-intervention effects, suggesting that the T1w/T2w is a sensitive metric to detect intervention effects.

#### **4.4. Processing speed and T1w/T2w**

Alterations in myelin and axonal properties can increase or decrease axonal conduction velocity, which has relevance to cognition (Fields, 2015). FA has been previously associated with processing speed ability (Borghesani et al., 2013; Burzynska et al., 2017) and the most common WM regions involved with processing speed are the prefrontal WM, FX, SLF and the uncinate fasciculus (Kennedy & Raz, 2009; Sasson, Doniger, Pasternak, Tarrasch, & Assaf, 2013). Decreased FA implies that some aspect of the WM microstructure is damaged, but changes in FA are dependent on numerous factors that are of functional relevance such as: fiber density, permeability of membranes and intra-voxel orientational coherence (Beaulieu, 2002; Jones et al., 2013). Therefore, it is not possible to specify how much a given change in anisotropy is due to changes in myelin content.

In our study, we observed that lower T1w/T2w values (in the whole WM) were predictors of decreased processing speed ability, after controlling for age, education and FA (in the whole WM). Even though, FA in the FX has been recognized as a significant predictor of processing speed in a previous study from this clinical trial (Burzynska et al., 2017), we were not able to observe this pattern for the T1w/T2w.

To our knowledge, there has been only one study of the association between T1w/T2w and processing speed ability that used the T1w/T2w ratio as a proxy of myelin content. In this study, Chopra and colleagues (2018), found that regions with high myelin content such as the ALIC and the left splenium of the CC were predictors of processing speed ability; however, total brain WM was not a significant predictor of processing speed. In spite of their large sample (277 middle-aged adults and 293 older adults), their older-age group ranged from 68-73 years, which could have restricted the variance associated with age-related WM deterioration (Chopra et al., 2018).

A possible explanation for the negative association between the T1w/T2s and processing speed is that, the highest T1w/T2w values were observed in deep WM regions, such as the internal capsule. These WM regions do not show consistent associations with processing speed ability, instead degeneration of the ALIC has shown to result in a subtle “disconnection syndrome” affecting executive functions (task-switching), while the PLIC comprises semantic and figural fluency measures (Sullivan, Zahr, Rohlfing, & Pfefferbaum, 2010). Another DTI study showed that processing speed ability was correlated with FA in the most anterior WM regions (PFC, reg1cc), while the ALIC and PLIC were associated with poorer episodic memory; however, this study did not include measures of verbal and nonverbal fluency failing to fully support the structure-function relations of the internal capsule (Kennedy & Raz, 2009). Our

results imply that the T1w/T2w has relevance for processing speed ability; however, this relationship should be further studied by looking at changes in specific WM regions and by studying the association of the T1w/T2w with other cognitive measures.

The association between processing speed ability has also been studied using myelin water fraction measures derived from multi-echo T2 relaxation analyses, which have been previously validated by histological measures of myelin (Laule et al., 2006). Interestingly, there was not a significant association between myelin water fraction and processing speed among cognitively healthy older adults (mean age=57); however, an index of axonal diameter (geomT2-IEW) was negatively associated with processing speed in the genu of the CC, suggesting that higher axonal density was associated with a positive change in processing speed (Arshad, 2017). Further studies by Raz and colleagues showed that the T1w/T2w was correlated with this index of axonal diameter ( $r = -.54, p < .05$ ), suggesting that the T1w/T2w could reflect changes in axonal diameter rather than myelin (Arshad, Stanley, & Raz, 2017; Hagiwara et al., 2018).

Even though, the study by Arshad (2017), was the first to test the hypothesis linking myelin content and processing speed, their results suggested a possible role of axon density rather than myelin content as a potential biological substrate. Still, the associations between myelin, axonal density and processing speed warrants further investigation.

#### **4.5. Associations between DTI and T1w/T2w**

Our results are consistent with the idea that T1w/T2w is less affected by crossing-fibers, since the associations between T1w/T2w and FA were stronger in regions with high orientational coherence, like the anterior corpus callosum, than in crossing-fiber regions. The most important determinant of the degree of anisotropy is the architecture of WM – how the axons are organized

within a voxel. In regions where the axons are aligned along the same axis and densely packed, we expect to see high FA, while regions with crossed fibers will have a lower FA, even with the same myelin content.

Some studies have provided evidence that changes in RD are associated with changes in the myelin sheath (Song et al., 2002a, 2005), or axon injury (Klawiter et al., 2011), but this is still disputed in the field (Wheeler-Kingshott & Cercignani, 2009). In our study, RD and the T1w/T2w were more strongly associated with each other in regions with higher myelin content such as the PLIC, ALIC and the reg3cc. However, one of our linear mixed models (PLIC vs. FX), should be evaluated carefully due to boundary issues of the estimated random-effects covariance matrix, that is, being singular or near singular, resulting in non-convergence. Future nonlinear optimization approaches would need to be taken to study these complex models.

#### **4.6. Correlations between T1w/T2w and age**

We also found evidence for the anterior-to-posterior gradient of WM deterioration, but this was more evident in FA than in T1w/T2w. We observed that FA was negatively correlated with age in most anterior regions of the corpus callosum but uncorrelated in the posterior regions. On the other hand, the T1w/T2w was negatively correlated with age in the medial region of the corpus callosum, where we expect to find larger axons with higher myelin content.

The most anterior region of the corpus callosum has high axonal density and a preponderance of smaller axons. In this region, about 20% of axons are unmyelinated. In contrast, the regions of the corpus callosum that project to the premotor, primary motor and primary sensory cortex have a lower density, but larger axons. Here, the ratio of unmyelinated axons is only about 10% (Lamantia & Rakic, 1990). This leads us to believe that the T1w/T2w

values near the middle of the corpus callosum reflect the larger mean diameter of axonal fibers and/or the concentration of myelin (Aboitiz et al., 1992b; Schneider et al., 2012b).

We examined the WM retrogenesis hypothesis by characterizing age-related differences in early- and late-myelinating regions for both FA and the T1w/T2w. FA had negative correlations with age in all late-myelinating regions, while this trend was not evident for the T1w/T2w. In contrast, we found that the T1w/T2w was positively correlated with age in both the PLIC (early-myelinating) and EC (late-myelinating). Our results are with agreement with a seven-year longitudinal DTI study, where Bender and colleagues, demonstrated that the PLIC is less vulnerable to age-related decline (Bender, Völkle, & Raz, 2016). However, WM lesions known as WM hyperintensities, increase in frequency with age and these are common in the PLIC and EC.

WM lesions appear as hypointense in comparison to normal appearing WM in T1-WIs, while they appear as hyperintense in T2-WIs. The difference in intensity signal in T1-WI and T2-WIs in the presence of WM lesions should lead to higher T1w/T2w values. WM hyperintensities have mostly been observed in regions within the deep and periventricular WM, such as the PLIC (Ketonen, 1998), but they can also be present in regions within the cholinergic WM pathway, such as the EC (Bocti et al., 2005). WM hyperintensities represent a continuous spectrum of WM injury, with damage to the WM tissue ranging from various degrees of demyelination to gliosis, arteriosclerosis and axonal loss (Gouw et al., 2011). Because the pathological substrates of WM hyperintensities are heterogeneous, the increased T1w/T2w values with age in the PLIC and the EC may be a reflection of increased WM lesions; however, these findings should be correlated with histopathology for further validation.

#### **4.7. Interpretation of the T1w/T2w signal. Is it myelin?**

The T1w/T2w signal may represent increase in axonal diameter, myelination or iron concentration, separately or in combination.

The T1w/T2w showed low to moderate correlations with myelin water fraction in previous studies; however, it has been associated with another index (geomT2IEW), which is a T2 relaxation component that corresponds to the water hindered between the intracellular and extracellular space, suggesting that this T2 relaxation component is more specific to axon diameter or axon packing density, rather than myelin (Arshad et al., 2017).

It has been shown that apart from myelin, iron and protein content can also affect T2\* decay (Duyn et al., 2007) and, iron and myelin co-localize in WM with similar T2 relaxation values (Langkammer et al., 2012). Iron accumulates as a function of the aging brain; however, very high iron levels (as seen in neurodegeneration) may lead to cell death via oxidative stress and pro-inflammatory mechanisms (Ndayisaba, Kaindlstorfer, & Wenning, 2019). Interestingly, oligodendrocytes have the largest intracellular stores of iron in the brain, which makes them the most vulnerable cell type to oxidative stress in the central nervous system (Bradl & Lassmann, 2010). Thus, high iron concentration can be a reflection of demyelination.

#### **4.8. Conclusions and limitations**

In conclusion, our study provides the first evidence for the T1w/T2w as a WM metric capable of detecting changes in WM after exercise lifestyle intervention. The current study; however, is not enough to determine whether the T1w/T2w is a meaningful predictor of cognitive function. The T1w/T2w ratio-processing speed relationship should be validated with myelin-specific measures. Furthermore, we found no evidence for the anterior-to-posterior

gradient and the retrogenesis hypothesis for the T1w/T2w when compared to FA, suggesting that DTI is more sensitive to general age differences in WM and that the T1w/T2w ratios and DTI appear to reflect different microstructural properties in the WM.

Finally, evidence from our study appears to indicate that the T1w/T2w is a measure of myelin content; however, the origin of the T1w/T2w signal is still unknown. We can only offer speculative explanations for the potential biological substrates of the T1w/T2w signal. However, because the T1w/T2w is highly accessible, does not require custom MRI sequences, has shown high concurrent validity after calibration procedures and offers greater ability than DTI to detect short-term longitudinal changes in WM, it offers a promising tool for longitudinal investigations of WM. Altogether, our data provides *in-vivo* evidence for WM plasticity using an accessible quantitative measure derived from the division of the T1-WI by the T2-WI. Further research is needed to gain a better understanding of its biological underpinnings and significance.

### **Limitations**

The TBSS analysis used here inherently focuses on normal appearing WM and the center of the tracts, that is because the highest FA values perpendicular to the tract are being projected to the WM skeleton for further analysis (Tract-Based Spatial Statistics, Smith et al., 2004, 2006, 2007). The TBSS pipeline may introduce bias by excluding some voxels affected by WM hyperintensities or by excluding part of the WM tracts that are not in the center.

### **Future directions**

Future analyses will need to elaborate on the ability of the T1w/T2w to detect changes in WM and cognition after lifestyle intervention. In future research, we will study: 1) whether the cardiorespiratory fitness levels predict the slope of the decline or increase in T1w/T2w over the

6-month period; 2) whether the T1w/T2w ratio is a significant predictor of other cognitive abilities other than processing speed; 3) whether the association between the T1w/T2w and processing speed is region specific; 4) whether the T1w/T2w is correlated with more specific myelin imaging methods and whether these associations differ in the ability to detect WM changes after intervention. 5) whether using multimodal fusion analyses would allow to integrate DTI with the T1w/T2w to characterize inter-subject variability attributed to the different modalities.

## REFERENCES

- Albin, E. E., Brellenthin, A. G., Lang, J. A., Meyer, J. D., & Lee, D. (2020). Cardiorespiratory Fitness and Muscular Strength on Arterial Stiffness in Older Adults. *Medicine & Science in Sports & Exercise*, 1. <https://doi.org/10.1249/mss.0000000000002319>
- Albinet, C. T., Boucard, G., Bouquet, C. A., & Audiffren, M. (2012). Processing speed and executive functions in cognitive aging: How to disentangle their mutual relationship? *Brain and Cognition*, 79(1), 1–11. <https://doi.org/10.1016/j.bandc.2012.02.001>
- Alexander, A. L., Lee, J. E., Lazar, M., & Field, A. S. (2007). Diffusion Tensor Imaging of the Brain. *Neurotherapeutics*, 4(3), 316–329. <https://doi.org/10.1016/j.nurt.2007.05.011>
- Arshad, M. (2017). Change In Processing Speed And Its Associations With Cerebral White Matter Microstructure. *Wayne State University Dissertations*. Retrieved from [https://digitalcommons.wayne.edu/oa\\_dissertations/1782](https://digitalcommons.wayne.edu/oa_dissertations/1782)
- Arshad, M., Stanley, J. A., & Raz, N. (2017). Test–retest reliability and concurrent validity of in vivo myelin content indices: Myelin water fraction and calibrated T1w/T2w image ratio. *Human Brain Mapping*, 38(4), 1780–1790. <https://doi.org/10.1002/hbm.23481>
- Barrick, T. R., Charlton, R. A., Clark, C. A., & Markus, H. S. (2010). White matter structural decline in normal ageing: A prospective longitudinal study using tract-based spatial statistics. *NeuroImage*, 51(2), 565–577. <https://doi.org/10.1016/J.NEUROIMAGE.2010.02.033>
- Bartzokis, G. (2004). Age-related myelin breakdown: a developmental model of cognitive decline and Alzheimer’s disease. *Neurobiology of Aging*, 25(1), 5–18.

<https://doi.org/10.1016/J.NEUROBIOLAGING.2003.03.001>

- Bartzokis, G., Lu, P. H., Tingus, K., Mendez, M. F., Richard, A., Peters, D. G., ... Mintz, J. (2010). Lifespan trajectory of myelin integrity and maximum motor speed. *Neurobiology of Aging*, *31*(9), 1554–1562. <https://doi.org/10.1016/j.neurobiolaging.2008.08.015>
- Basser, P. J., Mattiello, J., & LeBihan, D. (1994). MR diffusion tensor spectroscopy and imaging. *Biophysical Journal*, *66*(1), 259–267. [https://doi.org/10.1016/S0006-3495\(94\)80775-1](https://doi.org/10.1016/S0006-3495(94)80775-1)
- Beaulieu, C. (2002). The basis of anisotropic water diffusion in the nervous system - A technical review. *NMR in Biomedicine*, *15*(7–8), 435–455. <https://doi.org/10.1002/nbm.782>
- Behrens, T. E. J., Woolrich, M. W., Jenkinson, M., Johansen-Berg, H., Nunes, R. G., Clare, S., ... Smith, S. M. (2003). Characterization and Propagation of Uncertainty in Diffusion-Weighted MR Imaging. *Magn Reson Med*, *50*, 1077–1088. <https://doi.org/10.1002/mrm.10609>
- Bender, A. R., Völkle, M. C., & Raz, N. (2016). Differential aging of cerebral white matter in middle-aged and older adults: A seven-year follow-up. *NeuroImage*, *125*, 74–83. <https://doi.org/10.1016/J.NEUROIMAGE.2015.10.030>
- Bennett, I. J., & Madden, D. J. (2014, September 12). Disconnected aging: Cerebral white matter integrity and age-related differences in cognition. *Neuroscience*, Vol. 276, pp. 187–205. <https://doi.org/10.1016/j.neuroscience.2013.11.026>
- Bobinski, F., Martins, D. F., Bratti, T., Mazzardo-Martins, L., Winkelmann-Duarte, E. C., Guglielmo, L. G. A., & Santos, A. R. S. (2011). Neuroprotective and neuroregenerative

- effects of low-intensity aerobic exercise on sciatic nerve crush injury in mice. *Neuroscience*, 194, 337–348. <https://doi.org/10.1016/j.neuroscience.2011.07.075>
- Bocti, C., Swartz, R. H., Gao, F.-Q., Sahlas, D. J., Behl, P., & Black, S. E. (2005). A new visual rating scale to assess strategic white matter hyperintensities within cholinergic pathways in dementia. *Stroke*, 36(10), 2126–2131. <https://doi.org/10.1161/01.STR.0000183615.07936.b6>
- Booth, F. W., Roberts, C. K., & Laye, M. J. (2012). Lack of exercise is a major cause of chronic diseases. *Comprehensive Physiology*, 2(2), 1143–1211. <https://doi.org/10.1002/cphy.c110025>
- Borghesani, P. R., Madhyastha, T. M., Aylward, E. H., Reiter, M. A., Swarny, B. R., Warner Schaie, K., & Willis, S. L. (2013). The association between higher order abilities, processing speed, and age are variably mediated by white matter integrity during typical aging. *Neuropsychologia*, 51(8), 1435–1444. <https://doi.org/10.1016/j.neuropsychologia.2013.03.005>
- Bradl, M., & Lassmann, H. (2010, January). Oligodendrocytes: Biology and pathology. *Acta Neuropathologica*, Vol. 119, pp. 37–53. <https://doi.org/10.1007/s00401-009-0601-5>
- Brickman, A. M., Meier, I. B., Korgaonkar, M. S., Provenzano, F. A., Grieve, S. M., Siedlecki, K. L., ... Zimmerman, M. E. (2012). Testing the white matter retrogenesis hypothesis of cognitive aging. *Neurobiology of Aging*, 33(8), 1699–1715. <https://doi.org/10.1016/j.neurobiolaging.2011.06.001>
- Burzynska, A. Z., Chaddock-Heyman, L., Voss, M. W., Wong, C. N., Gothe, N. P., Olson, E. A., ... Kramer, A. F. (2014). Physical activity and cardiorespiratory fitness are beneficial for

white matter in low-fit older adults. *PLoS ONE*, 9(9).

<https://doi.org/10.1371/journal.pone.0107413>

Burzynska, A. Z., Garrett, D. D., Preuschhof, C., Nagel, I. E., Li, S.-C., Bäckman, L., ...

Lindenberger, U. (2013). A Scaffold for Efficiency in the Human Brain. *The Journal of Neuroscience*, 33(43), 17150 LP – 17159. [https://doi.org/10.1523/JNEUROSCI.1426-](https://doi.org/10.1523/JNEUROSCI.1426-13.2013)

13.2013

Burzynska, A. Z., Jiao, Y., Knecht, A. M., Fanning, J., Awick, E. A., Chen, T., ... Kramer, A. F.

(2017). White matter integrity declined over 6-months, but dance intervention improved integrity of the Fornix of older adults. *Frontiers in Aging Neuroscience*, 9(MAR).

<https://doi.org/10.3389/fnagi.2017.00059>

Burzynska, A. Z., Preuschhof, C., Bäckman, L., Nyberg, L., Li, S.-C., Lindenberger, U., &

Heekeren, H. R. (2010). Age-related differences in white matter microstructure: Region-specific patterns of diffusivity. *NeuroImage*, 49(3), 2104–2112.

<https://doi.org/10.1016/J.NEUROIMAGE.2009.09.041>

Chen, K., Zheng, Y., Wei, J. an, Ouyang, H., Huang, X., Zhang, F., ... Zhang, L. (2019).

Exercise training improves motor skill learning via selective activation of mTOR. *Science Advances*, 5(7), eaaw1888. <https://doi.org/10.1126/sciadv.aaw1888>

Chopra, S., Shaw, M., Shaw, T., Sachdev, P. S., Anstey, K. J., & Cherbuin, N. (2018). More

highly myelinated white matter tracts are associated with faster processing speed in healthy adults. *NeuroImage*, 171, 332–340. <https://doi.org/10.1016/j.neuroimage.2017.12.069>

Chorghay, Z., Káradóttir, R. T., & Ruthazer, E. S. (2018, November 16). White matter plasticity

keeps the brain in tune: Axons conduct while glia wrap. *Frontiers in Cellular Neuroscience*,

Vol. 12. <https://doi.org/10.3389/fncel.2018.00428>

Cohen, J. (1992). A power primer. *Psychological Bulletin*, *112*(1), 155–159.

<https://doi.org/10.1037/0033-2909.112.1.155>

Colcombe, Erickson, K. I., Scalf, P. E., Kim, J. S., Prakash, R., McAuley, E., ... Kramer, A. F. (2006). Aerobic Exercise Training Increases Brain Volume in Aging Humans. *The Journals of Gerontology: Series A*, *61*(11), 1166–1170. <https://doi.org/10.1093/gerona/61.11.1166>

Colcombe, S. J., Kramer, A. F., McAuley, E., Erickson, K. I., & Scalf, P. (2004). Neurocognitive aging and cardiovascular fitness: Recent findings and future directions. *Journal of Molecular Neuroscience*, *24*(1), 9–14. <https://doi.org/10.1385/jmn:24:1:009>

Craighead, D. H., Freeberg, K. A., & Seals, D. R. (2019, August 1). The protective role of regular aerobic exercise on vascular function with aging. *Current Opinion in Physiology*, Vol. 10, pp. 55–63. <https://doi.org/10.1016/j.cophys.2019.04.005>

Deoni, S. C. L. (2010). Quantitative relaxometry of the brain. *Topics in Magnetic Resonance Imaging*, *21*(2), 101–113. <https://doi.org/10.1097/RMR.0b013e31821e56d8>

Engvig, A., Fjell, A. M., Westlye, L. T., Moberget, T., Sundseth, Ø., Larsen, V. A., & Walhovd, K. B. (2012). Memory training impacts short-term changes in aging white matter: A Longitudinal Diffusion Tensor Imaging Study. *Human Brain Mapping*, *33*(10), 2390–2406. <https://doi.org/10.1002/hbm.21370>

Fields, R. D. (2015). A new mechanism of nervous system plasticity: activity-dependent myelination. *Nat Rev Neurosci*, *16*. <https://doi.org/10.1038/nrn4023>

Fleenor, B. S., Marshall, K. D., Durrant, J. R., Lesniewski, L. A., & Seals, D. R. (2010). Arterial

stiffening with ageing is associated with transforming growth factor- $\beta$ 1-related changes in adventitial collagen: Reversal by aerobic exercise. *Journal of Physiology*, 588(20), 3971–3982. <https://doi.org/10.1113/jphysiol.2010.194753>

Ganzetti, M., Wenderoth, N., & Mantini, D. (2014). Whole brain myelin mapping using T1- and T2-weighted MR imaging data. *Frontiers in Human Neuroscience*, 8, 671. <https://doi.org/10.3389/fnhum.2014.00671>

Ganzetti, M., Wenderoth, N., & Mantini, D. (2016). Intensity Inhomogeneity Correction of Structural MR Images: A Data-Driven Approach to Define Input Algorithm Parameters. *Frontiers in Neuroinformatics*, 10, 10. <https://doi.org/10.3389/fninf.2016.00010>

Garber, C. E., Blissmer, B., Deschenes, M. R., Franklin, B. A., Lamonte, M. J., Lee, I. M., ... Swain, D. P. (2011). Quantity and quality of exercise for developing and maintaining cardiorespiratory, musculoskeletal, and neuromotor fitness in apparently healthy adults: Guidance for prescribing exercise. *Medicine and Science in Sports and Exercise*, 43(7), 1334–1359. <https://doi.org/10.1249/MSS.0b013e318213fefb>

Glasser, M. F., & van Essen, D. C. (2011). Mapping human cortical areas in vivo based on myelin content as revealed by T1- and T2-weighted MRI. *Journal of Neuroscience*, 31(32), 11597–11616. <https://doi.org/10.1523/JNEUROSCI.2180-11.2011>

Gouw, A. A., Seewann, A., Van Der Flier, W. M., Barkhof, F., Rozemuller, A. M., Scheltens, P., & Geurts, J. J. G. (2011). Heterogeneity of small vessel disease: A systematic review of MRI and histopathology correlations. *Journal of Neurology, Neurosurgery and Psychiatry*, Vol. 82, pp. 126–135. <https://doi.org/10.1136/jnnp.2009.204685>

Gruber, B., Froeling, M., Leiner, T., & Klomp, D. W. J. (2018, September 1). RF coils: A

practical guide for nonphysicists. *Journal of Magnetic Resonance Imaging*, Vol. 48, pp. 590–604. <https://doi.org/10.1002/jmri.26187>

Grydeland, H., Walhovd, K. B., Tamnes, C. K., Westlye, L. T., & Fjell, A. M. (2013).

Intracortical myelin links with performance variability across the human lifespan: Results from T1- and T2- weighted MRI myelin mapping and diffusion tensor imaging. *Journal of Neuroscience*, 33(47), 18618–18630. <https://doi.org/10.1523/JNEUROSCI.2811-13.2013>

Gunning-Dixon, F. M., Brickman, A. M., Cheng, J. C., & Alexopoulos, G. S. (2009). Aging of cerebral white matter: A review of MRI findings. *International Journal of Geriatric Psychiatry*, Vol. 24, pp. 109–117. <https://doi.org/10.1002/gps.2087>

Hagiwara, A., Hori, M., Kamagata, K., Warntjes, M., Matsuyoshi, D., Nakazawa, M., ... Aoki, S. (2018). Myelin Measurement: Comparison between Simultaneous Tissue Relaxometry, Magnetization Transfer Saturation Index, and T1w/T2w Ratio Methods. *Scientific Reports*, 8(1). <https://doi.org/10.1038/s41598-018-28852-6>

Harkins, K. D., Xu, J., Dula, A. N., Li, K., Valentine, W. M., Gochberg, D. F., ... Does, M. D. (2016). The microstructural correlates of T1 in white matter. *Magnetic Resonance in Medicine*, 75(3), 1341–1345. <https://doi.org/10.1002/mrm.25709>

Head, D., Buckner, R. L., Shimony, J. S., Williams, L. E., Akbudak, E., Conturo, T. E., ... Snyder, A. Z. (2004). Differential Vulnerability of Anterior White Matter in Nondemented Aging with Minimal Acceleration in Dementia of the Alzheimer Type: Evidence from Diffusion Tensor Imaging. *Cerebral Cortex*, 14(4), 410–423. <https://doi.org/10.1093/cercor/bhh003>

Hillman, C. H., Erickson, K. I., & Kramer, A. F. (2008). Be smart, exercise your heart: exercise

effects on brain and cognition.(SCIENCE AND SOCIETY)(Report). *Nature Reviews Neuroscience*, 9(1), 58.

Hlavica, M., Delparente, A., Good, A., Good, N., Plattner, P. S., Seyedsadr, M. S., ... Ineichen, B. V. (2017). Intrathecal insulin-like growth factor 1 but not insulin enhances myelin repair in young and aged rats. *Neuroscience Letters*, 648, 41–46.

<https://doi.org/10.1016/j.neulet.2017.03.047>

Hofer, S., & Frahm, J. (2006). Topography of the human corpus callosum revisited- Comprehensive fiber tractography using diffusion tensor magnetic resonance imaging. *NeuroImage*, 32(3), 989–994. <https://doi.org/10.1016/j.neuroimage.2006.05.044>

Jack, C. R., Bernstein, M. A., Fox, N. C., Thompson, P., Alexander, G., Harvey, D., ... Weiner, M. W. (2008). The Alzheimer's disease neuroimaging initiative (ADNI): MRI methods. *Journal of Magnetic Resonance Imaging*, 27(4), 685–691.

<https://doi.org/10.1002/jmri.21049>

Jeurissen, B., Leemans, A., Jones, D. K., Tournier, J.-D., & Sijbers, J. (2011). Probabilistic fiber tracking using the residual bootstrap with constrained spherical deconvolution. *Human Brain Mapping*, 32(3), 461–479. <https://doi.org/10.1002/hbm.21032>

Johnson, N. F., Kim, C., Clasey, J. L., Bailey, A., & Gold, B. T. (2012). Cardiorespiratory fitness is positively correlated with cerebral white matter integrity in healthy seniors. *NeuroImage*, 59(2), 1514–1523. <https://doi.org/10.1016/j.neuroimage.2011.08.032>

Jones, D. K., Knösche, T. R., & Turner, R. (2013). White matter integrity, fiber count, and other fallacies: the do's and don'ts of diffusion MRI. *NeuroImage*, 73, 239–254.

<https://doi.org/10.1016/j.neuroimage.2012.06.081>

- Kennedy, K. M., & Raz, N. (2009). Aging white matter and cognition: Differential effects of regional variations in diffusion properties on memory, executive functions, and speed. *Neuropsychologia*, 47(3), 916–927. <https://doi.org/10.1016/j.neuropsychologia.2009.01.001>
- Ketonen, L. M. (1998). Neuroimaging of the aging brain. *Neurologic Clinics*, 16(3), 581–598. [https://doi.org/10.1016/S0733-8619\(05\)70082-7](https://doi.org/10.1016/S0733-8619(05)70082-7)
- Kinney, H. C., Ann brody, B., Kloman, A. S., & Gilles, F. H. (1988). Sequence of Central Nervous System Myelination in Human Infancy. II. Patterns of Myelination in Autopsied Infants. *Journal of Neuropathology and Experimental Neurology*, 47(3), 217–234. <https://doi.org/10.1097/00005072-198805000-00003>
- Kinney, H. C., & Volpe, J. J. (2018). Myelination Events. In *Volpe's Neurology of the Newborn* (pp. 176–188). <https://doi.org/10.1016/B978-0-323-42876-7.00008-9>
- Klawiter, E. C., Schmidt, R. E., Trinkaus, K., Liang, H. F., Budde, M. D., Naismith, R. T., ... Benzinger, T. L. (2011). Radial diffusivity predicts demyelination in ex vivo multiple sclerosis spinal cords. *NeuroImage*, 55(4), 1454–1460. <https://doi.org/10.1016/j.neuroimage.2011.01.007>
- Kochunov, P., Williamson, D. E., Lancaster, J., Fox, P., Cornell, J., Blangero, J., & Glahn, D. C. (2012). Fractional anisotropy of water diffusion in cerebral white matter across the lifespan. *Neurobiology of Aging*, 33(1), 9–20. <https://doi.org/10.1016/j.neurobiolaging.2010.01.014>
- Kuhn, S., Gritti, L., Crooks, D., & Dombrowski, Y. (2019). Oligodendrocytes in Development, Myelin Generation and Beyond. *Cells*, 8(11), 1424. <https://doi.org/10.3390/cells8111424>
- Lamantia, A. -S, & Rakic, P. (1990). Cytological and quantitative characteristics of four cerebral

commissures in the rhesus monkey. *Journal of Comparative Neurology*, 291(4), 520–537.  
<https://doi.org/10.1002/cne.902910404>

Langkammer, C., Krebs, N., Goessler, W., Scheurer, E., Yen, K., Fazekas, F., & Ropele, S. (2012). Susceptibility induced gray-white matter MRI contrast in the human brain. *NeuroImage*, 59(2), 1413–1419. <https://doi.org/10.1016/j.neuroimage.2011.08.045>

Laule, C., Leung, E., Li, D. K. B., Traboulsee, A. L., Paty, D. W., MacKay, A. L., & Moore, G. R. W. (2006). Myelin water imaging in multiple sclerosis: Quantitative correlations with histopathology. *Multiple Sclerosis*, 12(6), 747–753.  
<https://doi.org/10.1177/1352458506070928>

Lavin, K. M., Perkins, R. K., Jemiolo, B., Raue, U., Trappe, S. W., & Trappe, T. A. (2020). Effects of aging and lifelong aerobic exercise on basal and exercise-induced inflammation. *Journal of Applied Physiology (Bethesda, Md. : 1985)*, 128(1), 87–99.  
<https://doi.org/10.1152/jappphysiol.00495.2019>

Lebel, C., Gee, M., Camicioli, R., Wieler, M., Martin, W., & Beaulieu, C. (2012). Diffusion tensor imaging of white matter tract evolution over the lifespan. *NeuroImage*, 60(1), 340–352. <https://doi.org/10.1016/j.neuroimage.2011.11.094>

Lebel, C., Walker, L., Leemans, A., Phillips, L., & Beaulieu, C. (2008). Microstructural maturation of the human brain from childhood to adulthood. *NeuroImage*, 40(3), 1044–1055. <https://doi.org/10.1016/j.neuroimage.2007.12.053>

Lee, J. M., Park, J. M., Song, M. K., Oh, Y. J., Kim, C. J., & Kim, Y. J. (2017). The ameliorative effects of exercise on cognitive impairment and white matter injury from blood-brain barrier disruption induced by chronic cerebral hypoperfusion in adolescent rats. *Neuroscience*

*Letters*, 638, 83–89. <https://doi.org/10.1016/j.neulet.2016.12.018>

Lindenberger, U. (2014, October 31). Human cognitive aging: Corriger lafortune? *Science*, Vol. 346, pp. 572–578. <https://doi.org/10.1126/science.1254403>

Mädler, B., Drabycz, S. A., Kolind, S. H., Whittall, K. P., & MacKay, A. L. (2008). Is diffusion anisotropy an accurate monitor of myelination?. Correlation of multicomponent T2 relaxation and diffusion tensor anisotropy in human brain. *Magnetic Resonance Imaging*, 26(7), 874–888. <https://doi.org/10.1016/j.mri.2008.01.047>

Marner, L., Nyengaard, J. R., Tang, Y., & Pakkenberg, B. (2003). Marked loss of myelinated nerve fibers in the human brain with age. *Journal of Comparative Neurology*, 462(2), 144–152. <https://doi.org/10.1002/cne.10714>

Mason, J. L., Langaman, C., Morell, P., Suzuki, K., & Matsushima, G. K. (2001). Episodic demyelination and subsequent remyelination within the murine central nervous system: Changes in axonal calibre. *Neuropathology and Applied Neurobiology*, 27(1), 50–58. <https://doi.org/10.1046/j.0305-1846.2001.00301.x>

Moody, D. M., Bell, M. A., & Challa, V. R. (1990). Features of the cerebral vascular pattern that predict vulnerability to perfusion or oxygenation deficiency: An anatomic study. *American Journal of Neuroradiology*, 11(3), 431–439.

Nakamura, K., Chen, J. T., Ontaneda, D., Fox, R. J., & Trapp, B. D. (2017). T1-/T2-weighted ratio differs in demyelinated cortex in multiple sclerosis. *Annals of Neurology*, 82(4), 635–639. <https://doi.org/10.1002/ana.25019>

Ndayisaba, A., Kaindlstorfer, C., & Wenning, G. K. (2019, March 1). Iron in neurodegeneration

- Cause or consequence? *Frontiers in Neuroscience*, Vol. 13, p. 180.

<https://doi.org/10.3389/fnins.2019.00180>

O’Sullivan, M., Jones, D. K., Summers, P. E., Morris, R. G., Williams, S. C. R., & Markus, H. S.

(2001). Evidence for cortical “disconnection” as a mechanism of age-related cognitive decline. *Neurology*, 57(4), 632–638. <https://doi.org/10.1212/WNL.57.4.632>

Oberlin, L. E., Verstynen, T. D., Burzynska, A. Z., Voss, M. W., Prakash, R. S., Chaddock-

Heyman, L., ... Erickson, K. I. (2016). White matter microstructure mediates the relationship between cardiorespiratory fitness and spatial working memory in older adults. *NeuroImage*, 131, 91–101. <https://doi.org/10.1016/j.neuroimage.2015.09.053>

Oishi, K., Faria, A. V., & van Zijl, P. C. M. (2012). *MRI Atlas of Human White Matter (2)*.

Academic Press.

Peters, A. (2002a). Structural changes that occur during normal aging of primate cerebral hemispheres. *Neuroscience and Biobehavioral Reviews*, 26(7), 733–741.

[https://doi.org/10.1016/S0149-7634\(02\)00060-X](https://doi.org/10.1016/S0149-7634(02)00060-X)

Peters, A. (2002b, September). The effects of normal aging on myelin and nerve fibers: A review. *Journal of Neurocytology*, Vol. 31, pp. 581–593.

<https://doi.org/10.1023/A:1025731309829>

Peters, A., Sethares, C., & Moss, M. B. (2010). How the primate fornix is affected by age. *The*

*Journal of Comparative Neurology*, 518(19), 3962–3980. <https://doi.org/10.1002/cne.22434>

Pierpaoli, C., & Basser, P. J. (1996). Toward a quantitative assessment of diffusion anisotropy.

*Magnetic Resonance in Medicine*, 36(6), 893–906.

<https://doi.org/10.1002/mrm.1910360612>

Raz, N., Lindenberger, U., Rodrigue, K. M., Kennedy, K. M., Head, D., Williamson, A., ...

Acker, J. D. (2005). Regional brain changes in aging healthy adults: general trends, individual differences and modifiers. *Cerebral Cortex*, *15*(11), 1676–1689. Retrieved from <http://citeseerx.ist.psu.edu/viewdoc/summary?doi=10.1.1.318.1885>

Reisberg, B., Franssen, E. H., Hasan, S. M., Monteiro, I., Boksay, I., Souren, L. E. M., ...

Kluger, A. (1999). Retrogenesis: Clinical, physiologic, and pathologic mechanisms in brain aging, Alzheimer's and other dementing processes. *European Archives of Psychiatry and Clinical Neuroscience*, *249*(SUPPL. 3). <https://doi.org/10.1007/pl00014170>

Rektorova, I., Klobusiakova, P., Balazova, Z., Kropacova, S., Sejnoha Minsterova, A., Grmela,

R., ... Rektor, I. (2020). Brain structure changes in nondemented seniors after six-month dance-exercise intervention. *Acta Neurologica Scandinavica*, *141*(1), 90–97.

<https://doi.org/10.1111/ane.13181>

Rodrigue, K. M., & Kennedy, K. M. (2011). The Cognitive Consequences of Structural Changes to the Aging Brain. In *Handbook of the Psychology of Aging* (pp. 73–91).

<https://doi.org/10.1016/B978-0-12-380882-0.00005-X>

Rueckert, D. (1999). Nonrigid registration using free-form deformations: Application to breast mr images. *IEEE Transactions on Medical Imaging*, *18*(8), 712–721.

<https://doi.org/10.1109/42.796284>

Salat, D. H., Tuch, D. S., Greve, D. N., van der Kouwe, A. J. W., Hevelone, N. D., Zaleta, A. K., ...

... Dale, A. M. (2005). Age-related alterations in white matter microstructure measured by diffusion tensor imaging. *Neurobiology of Aging*, *26*(8), 1215–1227.

<https://doi.org/10.1016/j.neurobiolaging.2004.09.017>

Salthouse, T. A. (1985). *A theory of cognitive aging*. North-Holland.

Salthouse, T. A. (1996). The processing-speed theory of adult age differences in cognition.

*Psychological Review*, 103(3), 403–428. Retrieved from

<http://www.ncbi.nlm.nih.gov/pubmed/8759042>

Sampaio-Baptista, C., & Johansen-Berg, H. (2017, December 20). White Matter Plasticity in the Adult Brain. *Neuron*, Vol. 96, pp. 1239–1251. <https://doi.org/10.1016/j.neuron.2017.11.026>

Sasson, E., Doniger, G. M., Pasternak, O., Tarrasch, R., & Assaf, Y. (2013). White matter correlates of cognitive domains in normal aging with diffusion tensor imaging. *Frontiers in Neuroscience*, 7(7 MAR), 32. <https://doi.org/10.3389/fnins.2013.00032>

Scheltens, P., Barkhof, F., Leys, D., Wolters, E. C., Ravid, R., & Kamphorst, W. (1995). Histopathologic correlates of white-matter changes on MRI in alzheimer's disease and normal aging. *Neurology*, 45(5), 883–888. <https://doi.org/10.1212/WNL.45.5.883>

Schoenemann, P. T., Sheehan, M. J., & Glotzer, L. D. (2005). Prefrontal white matter volume is disproportionately larger in humans than in other primates. *Nature Neuroscience*, 8(2), 242–252. <https://doi.org/10.1038/nn1394>

Sharma, H. A., & Lagopoulos, J. (2010). MRI physics: pulse sequences. *Acta Neuropsychiatrica*, 22(2), 90–92. <https://doi.org/10.1111/j.1601-5215.2010.00449.x>

Sherwood, C. C., Gordon, A. D., Allen, J. S., Phillips, K. A., Erwin, J. M., Hof, P. R., & Hopkins, W. D. (2011). Aging of the cerebral cortex differs between humans and chimpanzees. *Proceedings of the National Academy of Sciences of the United States of*

*America*, 108(32), 13029–13034. <https://doi.org/10.1073/pnas.1016709108>

Shi, Y., & Wardlaw, J. M. (2016, September 1). Update on cerebral small vessel disease: A dynamic whole-brain disease. *Stroke and Vascular Neurology*, Vol. 1, pp. 83–92.

<https://doi.org/10.1136/svn-2016-000035>

Simon, C., Götz, M., & Dimou, L. (2011). Progenitors in the adult cerebral cortex: Cell cycle properties and regulation by physiological stimuli and injury. *GLIA*, 59(6), 869–881.

<https://doi.org/10.1002/glia.21156>

Slater, D. A., Melie-Garcia, L., Preisig, M., Kherif, F., Lutti, A., & Draganski, B. (2019). Evolution of white matter tract microstructure across the life span. *Human Brain Mapping*, 40(7), 2252–2268. <https://doi.org/10.1002/hbm.24522>

Smith, S. M., Jenkinson, M., Johansen-Berg, H., Rueckert, D., Nichols, T. E., Mackay, C. E., ... Behrens, T. E. J. (2006). Tract-based spatial statistics: Voxelwise analysis of multi-subject diffusion data. *NeuroImage*, 31(4), 1487–1505.

<https://doi.org/10.1016/j.neuroimage.2006.02.024>

Song, S. K., Sun, S.-W., Ju, W.-K., Lin, S.-J., Cross, A. H., & Neufeld, A. H. (2003). Diffusion tensor imaging detects and differentiates axon and myelin degeneration in mouse optic nerve after retinal ischemia. *NeuroImage*, 20(3), 1714–1722.

<https://doi.org/10.1016/j.neuroimage.2003.07.005>

Song, S. K., Sun, S., Ramsbottom, M. J., Chang, C., Russell, J., & Cross, A. H. (2002a). *Dysmyelination Revealed through MRI as Increased Radial ( but Unchanged Axial )*

*Diffusion of Water*. 1436, 1429–1436. <https://doi.org/10.1006/nimg.2002.1267>

- Song, S. K., Sun, S. W., Ramsbottom, M. J., Chang, C., Russell, J., & Cross, A. H. (2002b). Demyelination revealed through MRI as increased radial (but unchanged axial) diffusion of water. *NeuroImage*, *17*(3), 1429–1436. <https://doi.org/10.1006/nimg.2002.1267>
- Song, S. K., Yoshino, J., Le, T. Q., Lin, S. J., Sun, S. W., Cross, A. H., & Armstrong, R. C. (2005). Demyelination increases radial diffusivity in corpus callosum of mouse brain. *NeuroImage*, *26*(1), 132–140. <https://doi.org/10.1016/j.neuroimage.2005.01.028>
- Sullivan, E. V., Rohlfing, T., & Pfefferbaum, A. (2010a). Quantitative fiber tracking of lateral and interhemispheric white matter systems in normal aging: Relations to timed performance. *Neurobiology of Aging*, *31*(3), 464–481. <https://doi.org/10.1016/j.neurobiolaging.2008.04.007>
- Sullivan, E. V., Zahr, N. M., Rohlfing, T., & Pfefferbaum, A. (2010). Fiber tracking functionally distinct components of the internal capsule. *Neuropsychologia*, *48*(14), 4155–4163. <https://doi.org/10.1016/j.neuropsychologia.2010.10.023>
- Sullivan, E. V., Rohlfing, T., & Pfefferbaum, A. (2010b). Longitudinal study of callosal microstructure in the normal adult aging brain using quantitative DTI fiber tracking. *Developmental Neuropsychology*, *35*(3), 233–256. <https://doi.org/10.1080/87565641003689556>
- Tan, C. H., Low, K. A., Chiarelli, A. M., Fletcher, M. A., Navarra, R., Burzynska, A. Z., ... Fabiani, M. (2019). Optical measures of cerebral arterial stiffness are associated with white matter signal abnormalities and cognitive performance in normal aging. *Neurobiology of Aging*, *84*, 200–207. <https://doi.org/10.1016/j.neurobiolaging.2019.08.004>
- Tournier, J.-D., Mori, S., & Leemans, A. (2011). Diffusion tensor imaging and beyond. *Magnetic*

*Resonance in Medicine*, 65(6), 1532–1556. <https://doi.org/10.1002/mrm.22924>

Tse, K. H., & Herrup, K. (2017). DNA damage in the oligodendrocyte lineage and its role in brain aging. *Mechanisms of Ageing and Development*, 161(Pt A), 37–50.

<https://doi.org/10.1016/j.mad.2016.05.006>

Tseng, B. Y., Gundapuneedi, T., Khan, M. A., Diaz-Arrastia, R., Levine, B. D., Lu, H., ...

Zhang, R. (2013). White matter integrity in physically fit older adults. *NeuroImage*, 82,

510–516. <https://doi.org/10.1016/j.neuroimage.2013.06.011>

Uddin, M. N., Figley, T. D., Marrie, R. A., & Figley, C. R. (2018). Can T1w/T2w ratio be used as a myelin-specific measure in subcortical structures? Comparisons between FSE-based

T1w/T2w ratios, GRASE-based T1w/T2w ratios and multi-echo GRASE-based myelin

water fractions. *NMR in Biomedicine*, 31(3). <https://doi.org/10.1002/nbm.3868>

Vincze, A., Mázló, M., Seress, L., Komoly, S., & Ábrahám, H. (2008). A correlative light and electron microscopic study of postnatal myelination in the murine corpus callosum.

*International Journal of Developmental Neuroscience*, 26(6), 575–584.

<https://doi.org/10.1016/j.ijdevneu.2008.05.003>

Voss, M. W., Heo, S., Prakash, R. S., Erickson, K. I., Alves, H., Chaddock, L., ... Kramer, A. F.

(2013). The influence of aerobic fitness on cerebral white matter integrity and cognitive

function in older adults: Results of a one-year exercise intervention. *Human Brain Mapping*,

34(11), 2972–2985. <https://doi.org/10.1002/hbm.22119>

Voss, M. W., Weng, T. B., Burzynska, A. Z., Wong, C. N., Cooke, G. E., Clark, R., ... Kramer,

A. F. (2016). Fitness, but not physical activity, is related to functional integrity of brain

networks associated with aging. *NeuroImage*, 131, 113–125.

<https://doi.org/10.1016/j.neuroimage.2015.10.044>

Washida, K., Hattori, Y., & Ihara, M. (2019). Animal Models of Chronic Cerebral Hypoperfusion: From Mouse to Primate. *International Journal of Molecular Sciences*, *20*(24), 6176. <https://doi.org/10.3390/ijms20246176>

Wassenaar, T. M., Yaffe, K., van der Werf, Y. D., & Sexton, C. E. (2019). Associations between modifiable risk factors and white matter of the aging brain: insights from diffusion tensor imaging studies. *Neurobiology of Aging*, *80*, 56–70. <https://doi.org/10.1016/j.neurobiolaging.2019.04.006>

Wheeler-Kingshott, C. A. M., & Cercignani, M. (2009). About “axial” and “radial” diffusivities. *Magnetic Resonance in Medicine*, *61*(5), 1255–1260. <https://doi.org/10.1002/mrm.21965>

Yagishita, A., Nakano, I., Oda, M., & Hirano, A. (1994). Location of the corticospinal tract in the internal capsule at MR imaging. *Radiology*, *191*(2), 455–460. <https://doi.org/10.1148/radiology.191.2.8153321>

APPENDIX A

**Appendix A. Correlations between FA values from the current sample vs. original sample**

<b>ROI</b>		<b>Pre-intervention</b>	<b>Post-intervention</b>
<b>ACC</b>	Pearson's r	.998**	.998**
<b>ALIC</b>	Pearson's r	.999**	.999**
<b>CC</b>	Pearson's r	1.000**	1.000**
<b>EC</b>	Pearson's r	.999**	.999**
<b>FX</b>	Pearson's r	.999**	.999**
<b>PLIC</b>	Pearson's r	1.000**	1.000**
<b>prefrontal</b>	Pearson's r	.999**	.999**
<b>reg1cc</b>	Pearson's r	.999**	1.000**
<b>reg2cc</b>	Pearson's r	1.000**	1.000**
<b>reg3cc</b>	Pearson's r	1.000**	1.000**
<b>reg4cc</b>	Pearson's r	.999**	.999**
<b>reg5cc</b>	Pearson's r	.999**	.999**
<b>SCR</b>	Pearson's r	.999**	.999**
<b>SLF</b>	Pearson's r	.999**	1.000**

\*\* . Correlation is significant at the 0.01 level.

\* . Correlation is significant at the 0.05 level.

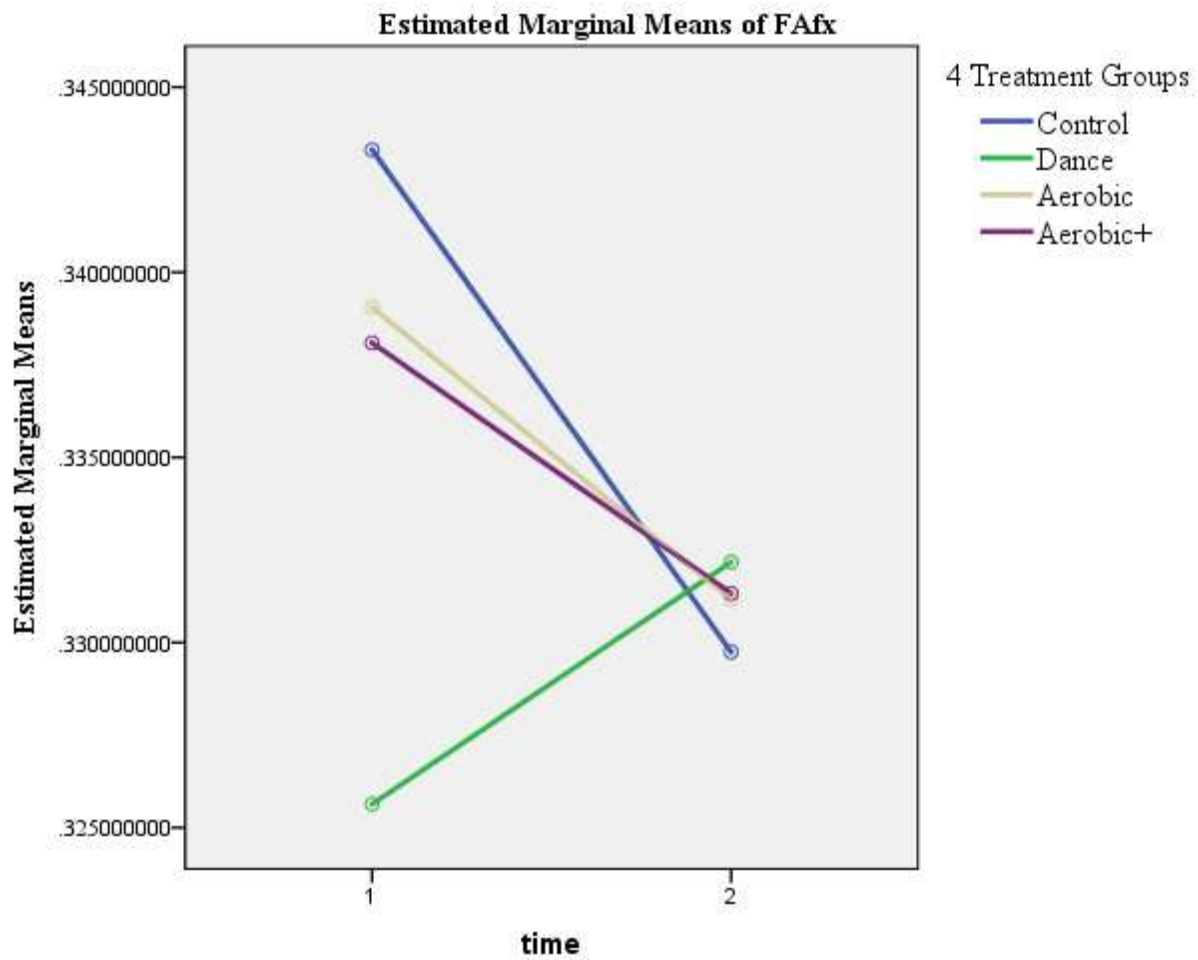
APPENDIX B

**Appendix B. Time-by-intervention interactions for the T1w/T2w**

*Fixed effect for the interaction term*

<b>ROI</b>	<b><math>\beta</math></b>	<b><i>p</i> value</b>	<b>Std. Error</b>
Total WM			
Time-by-treatment reg1cc	0.31	0.010	0.12
Time-by-treatment reg2cc	0.24	<b>0.014</b>	0.09
Time-by-treatment reg3cc	0.07	0.173	0.05
Time-by-treatment reg4cc	0.05	0.232	0.04
Time-by-treatment reg5cc	0.05	0.162	0.03
Time-by-treatment PLIC	0.17	<b>0.003</b>	0.05
Time-by-treatment ALIC	0.27	<b>0.002</b>	0.08
Time-by-treatment SCR	0.33	<b>0.001</b>	0.09
Time-by-treatment EC	0.18	0.095	0.11
Time-by-treatment SLF	0.09	0.187	0.07
Time-by-treatment FX	0.21	<b>0.037</b>	0.10
Time-by-treatment Prefrontal	0.02	0.632	0.01
Time-by-treatment	0.22	<b>0.043</b>	0.10

## APPENDIX C



**Appendix C. Results from repeated measures ANOVA showing significant time-by-intervention interaction only in the fornix for FA.**

Note: Time-by-intervention interaction in FA in the fornix in the four intervention groups.